TISSUE ENGINEERING: Part A
Volume 20, Numbers 3 and 4, 2014

DOI: 10.1089/ten.tea.2013.0053

Original Articles

Implantation of a Novel Biologic and Hybridized Tissue Engineered Bioimplant in Large Tendon Defect: An *In Vivo* Investigation

Ahmad Oryan, DVM, PhD,[1] Ali Moshiri, DVM, DVSc,[2] Abdolhamid Meimandi Parizi, DVM, PhD,[2] and Nicola Maffulli, MD, MS, PhD, FRCP, FRCS (Orth), FFSEM[3,4]

Surgical reconstruction of large Achilles tendon defects is technically demanding. There is no standard method, and tissue engineering may be a valuable option. We investigated the effects of 3D collagen and collagen-polydioxanone sheath (PDS) implants on a large tendon defect model in rabbits. Ninety rabbits were divided into three groups: control, collagen, and collagen-PDS. In all groups, 2 cm of the left Achilles tendon were excised and discarded. A modified Kessler suture was applied to all injured tendons to retain the gap length. The control group received no graft, the treated groups were repaired using the collagen only or the collagen-PDS prostheses. The bioelectrical characteristics of the injured areas were measured at weekly intervals. The animals were euthanized at 60 days after the procedure. Gross, histopathological and ultrastructural morphology and biophysical characteristics of the injured and intact tendons were investigated. Another 90 pilot animals were also used to investigate the inflammatory response and mechanism of graft incorporation during tendon healing. The control tendons showed severe hyperemia and peritendinous adhesion, and the gastrocnemius muscle of the control animals showed severe atrophy and fibrosis, with a loose areolar connective tissue filling the injured area. The tendons receiving either collagen or collagen-PDS implants showed lower amounts of peritendinous adhesion, hyperemia and muscle atrophy, and a dense tendon filled the defect area. Compared to the control tendons, application of collagen and collagen-PDS implants significantly improved water uptake, water delivery, direct transitional electrical current and tissue resistance to direct transitional electrical current. Compared to the control tendons, both prostheses showed significantly increased diameter, density and alignment of the collagen fibrils and maturity of the tenoblasts at ultrastructure level. Both prostheses influenced favorably tendon healing compared to the control tendons, with no significant differences between collagen and collagen-PDS groups. Implantation of the 3D collagen and collagen-PDS implants accelerated the production of a new tendon in the defect area, and may become a valuable option in clinical practice.

Introduction

The management of tendon injury with tissue loss is challenging.[1–3] Low healing rates, development of peritendinous adhesions and muscle atrophy are major consequences.[4–7] Direct suturing of such tendons may not be possible, and tendon transfer or lengthening can be technically demanding and of uncertain outcome.[4,8–11] In these injuries, tendon grafting has been used.[3,12,13] Both auto and allografts have limitations, including availability of grafts, cosmetic and functional donor site morbidity, technical demands, rejection, transmissible viral diseases, ethics concerns, and costs.[9,12,14]

Xenografts are an option, but there are concerns of acute rejection and disease transmission.[9,15–18] Tissue engineering is an option to consider in such instances,[19–21] although most investigations have focused on *in vitro* experimentation.[19] Therefore, most of the commercial tissue engineered products have produced dubious results *in vivo*, and the immunological reactions after implantation of these products are unclear.[16,19,22] In addition, the healing response of tissue engineered products *in vivo* is not comprehensively investigated.[19]

Tissue engineered products could be divided into biologic, synthetic, and hybrid implants.[9,17,19] Most biologic scaffolds are xenogenic, and most processing methods on these scaffolds

[1]Department of Pathology, School of Veterinary Medicine, Shiraz University, Shiraz, Iran.
[2]Division of Surgery, Department of Clinical Sciences, School of Veterinary Medicine, Shiraz University, Shiraz, Iran.
[3]Department of Musculoskeletal Medicine and Surgery, Faculty of Medicine and Surgery, University of Salerno, Salerno, Italy.
[4]Centre for Sport and Exercise Medicine, Barts and the London School of Medicine and Dentistry, University of London, Queen Mary, United Kingdom.

involve decellularization of the tissues.[15] Thus, these types of scaffolds are not specific for a particular molecule (e.g., collagen).[15,20] Therefore, the architecture of such tridimensional[19] scaffolds is not altered by the tissue engineering technologies.[9] *In vivo*, these implants did not improve the characteristics of the healing tissue, and the rate of rejection can be high.[15]

The use of synthetic scaffolds has been accompanied by severe inflammatory response, and the presence of toxic degradable products.[19] Also, their architecture is mainly bidimensional.[19] However, scaffolds can be fabricated in several manners, and their architecture could be manipulated so that they could be more appropriate for tissue regeneration. These scaffolds have been combined with biological products to decrease the amount of synthetic material in the scaffolds and to produce appropriate tridimensional structures.[9]

Ideally, scaffolds should be biodegradable and biocompatible, and their architecture is able to accelerate cell migration and proliferation and enhance tissue regeneration *in vivo*.[23] Collagen molecules are the major constituent of tendons, and they are polymerized as fibrils, fibers, fiber bundles and fascicles.[24–26] These unique structures are covered with paratenon or tenosynovium, which prevent adhesion formation after injury and facilitate tendon movement.[24,27]

We constructed a novel tridimensional collagen implant with or without a covering synthetic bidimensional scaffold. The effectiveness of these scaffolds on large tendon defect model in rabbits was investigated in terms of gross morphology, light microscopy and ultrastructural, biophysical, bioelectrical and biomechanical properties. We hypothesized that this novel tridimensional collagen implant is biodegradable and biocompatible, and increases the number, diameter, density and alignment of the newly regenerated collagen fibrils and fibers. These structural developments improve the biophysical and bioelectrical characteristics of the newly regenerated tendon. The covering bidimensional synthetic scaffold may have a role in decreasing the peritendinous adhesion, muscle and tendon atrophy. Therefore, combining such a bidimensional scaffold with a tridimensional collagen implant may increase the quality of the newly regenerated tissue in the defect area.

Materials and Methods

Ethics

The investigators who undertook the measurements and analyses of the results were unaware of the experimental design and grouping details. All animals received humane care in compliance with the Guide for Care and Use of Laboratory Animals published by the National Institutes of Health (NIH publication No. 85-23, revised 1985). The animals were housed in individual standard rabbit cages and maintained on standard rabbit diet, with no limitation of access to food or water. The study was approved by the local Ethics Committee of our faculty.

Study design

This study was a controlled laboratory study. One hundred and eighty skeletally-mature male White New Zealand rabbits aged 12 ± 2 months and 3.14 ± 0.17 kg body mass were randomly divided into treated collagen ($n = 60$), treated collagen-polydioxanone sheath (PDS) ($n = 60$), and control ($n = 60$) groups. The left Achilles tendon of each animal in all groups was designated as the transected/injured tendon, and the right, normal contra-lateral tendon (NCT) was left intact. In each group, the animals were randomly divided into two subgroups of experimental ($n = 30$) and pilot ($n = 30$) animals.

The bioelectrical characteristics of the injured and normal tendons of the experimental animals were investigated weekly, and the animals were euthanized 60 days post injury (DPI). Their tendons were investigated morphologically and biophysically. The pilot animals of each group ($n = 30$) were randomly divided into six pilot groups with five rabbits each. The animals in the pilot groups were euthanized at 6, 12, 18, 24, 30 and 40 DPI, and their injured tendons ($n = 5$ for each group) were histologically examined.

Preparation of the collagen implant

Collagen type I was extracted from the bovine superficial digital flexor tendon as previously described.[28] The acid solubilized collagen molecules were electrospinned onto a dual plate device to produce the large and aligned electrospun collagen fibers.[29] After electrospinning, the acid-solubilized bovine tendon type I collagen molecules were mixed with electrospun collagen fibers and polymerized in an incubator at 4°C for 48 h to produce tridimensional collagen gel. The type I collagen fibers were aligned under 12 Tesla magnetic fields (CRETA) during polymerization.[30] The electrospun collagen matrix (2D) acted as a core with its fibro-conductive characteristics and improved alignment of the newly formed collagen fibers. The collagen composite was cut into several pieces of the same size and shape as the rabbit's Achilles apparatus (L = 2 cm, H = 3.5 mm, W = 3 mm). The collagen composites were cross-linked after suspension in iso-osmolar 0.1% riboflavin solution, using UV (wavelength of 365 nm) irradiation.[31] To produce the bio-synthetic implant, polydioxanon nano scaled plates were purchased (PDS plate; Ethicon, Johnson & Johnson), sectioned at 300 nm, melted and wrapped around each collagen piece to cover the implant at the periphery. The final product was repeatedly washed with distilled water, and received 100 Gray g-radiation, and was suspended in 96% ethanol to produce and maintain sterility until surgery[32] (Fig. 1).

Initial tests of the scaffolds

The purity of the type I collagen was confirmed by sodium dodecyl sulfate poly-acrylamide gel electrophores.[28] The morphology of the scaffold was studied by scanning electron microscopy (SEM). Sterility and endotoxin content were tested and confirmed by microbiological and limulus amebocyte lysate test respectively *in vitro*.[33] The scaffolds were seeded using rat skin fibroblasts (cell line CRL-1213), and cell viability was determined and confirmed by histology, SEM and live/dead cell assay[34] (Fig. 2).

Premedication and anesthesia

The animals were premedicated by intra-muscular (IM) injection of 1 mg/kg acepromazine maleate, and were anesthetized by IM injection of 30 mg/kg Ketamine combined with 0.05 mg/kg Xylazine hydrochloride.[27]

Injury induction and surgical reconstruction

Under aseptic conditions, a lateral longitudinal incision was made on the skin over the left Achilles tendon. A skin

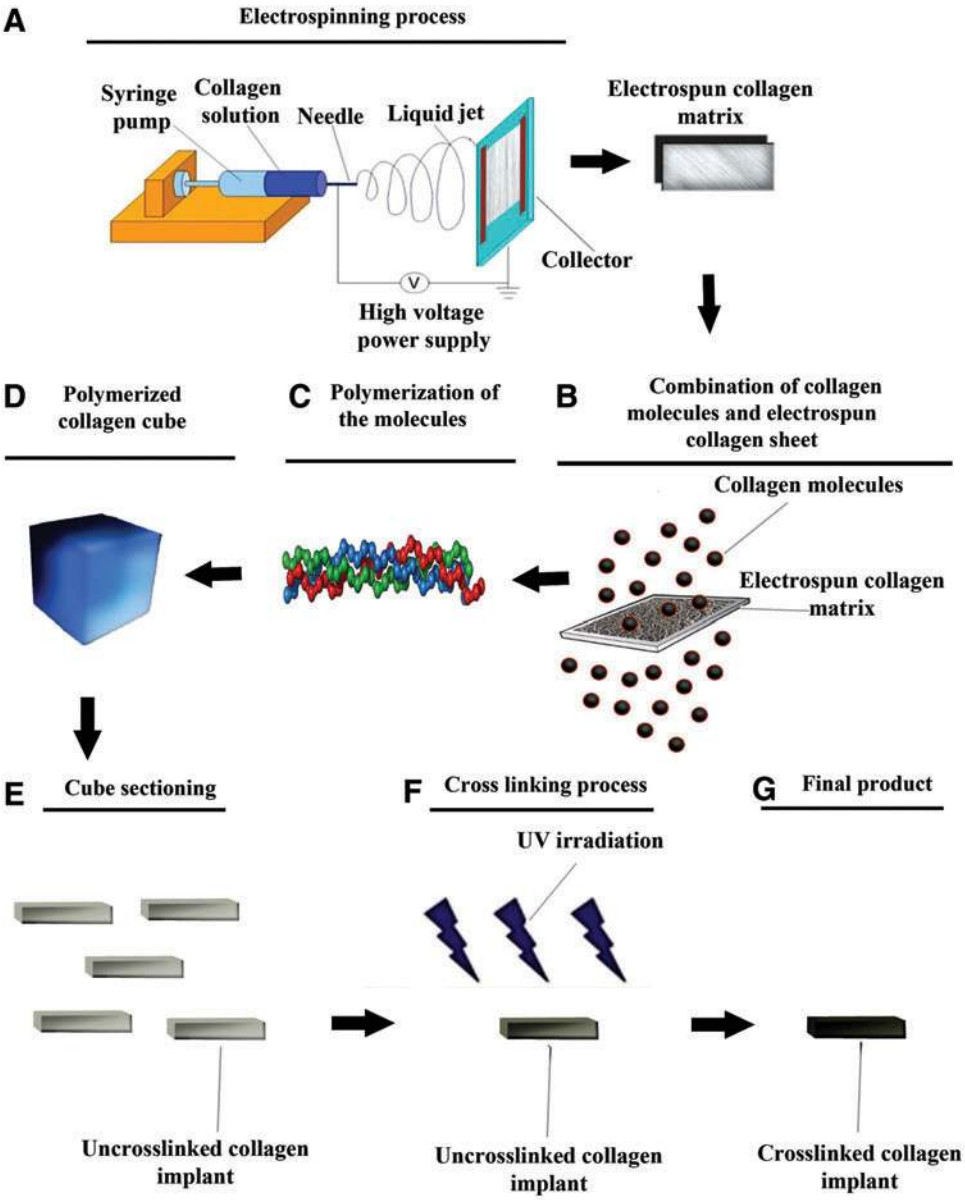

FIG. 1. Preparation of the collagen implant. The collagen solution was placed in the syringe pump with the needle charged at 6 kV with respect to the base plate **(A)**. The nanofibers were harvested and mixed with fresh collagen solution **(B)**, incubated for final polymerization **(C)**. This hybridized collagen gel was dried **(D)** and cut into rectangular strips to form several prostheses **(E)** which were crosslinked **(F)**, sterilized and then dried **(G)**. Each arrow shows a next step **(A–G)**. Color images available online at www.liebertpub.com/tea

flap was reflected medially to expose the Achilles tendon. Two cm of the Achilles tendon with its paratenon were excised (~70% of the Achilles tendon), from ~0.5 cm distal to the gastrocnemius muscle to 0.5 cm proximal to the calcaneal tuberosity. Primary realignment of the tendon extremities was undertaken using double stranded monofilament absorbable polydioxanon 0–4 suture material and a straight taper-cut orthopedic needle (PDS; Ethicon, Inc., 1997, Johnson & Johnson), in a modified Kessler core pattern, to arrange the edges of the tendon into a normal anatomical orientation but leaving a 2 cm gap between the extremities.[2,35] This method was applied for the control and treated groups. In each treated animal, the implant was implanted in the tendon gap, and a double-stranded suture was routed through the longitudinal axis of the prosthetic implant. The skin over the lesion was closed using 2-0 silk in a continuous pattern. All surgical procedures were undertaken by one experienced surgeon. No prosthesis was used in the control tendons (left injured control tendon [ICT]), and the gap was left intact. In the defect areas of the rabbits of the collagen implant group, the tridimensional collagen prosthesis (injured treated tendons with collagen prosthesis [ITTC]) was implanted. In the defect areas of the rabbits of the treated collagen-PDS group, the bio-synthetic tridimensional collagen implants (injured treated tendons with collagen-polydioxanon prosthesis [ITTC-PDS]) covered with the bidimensional polydioxanon scaffolds was implanted. Postoperative analgesia with fentanyl (Matrifen, Roskilde, DK; 0.0015 mg/kg/h) was provided for 3 DPI via a transdermal patch applied to the shaven and sutured skin. Given the strict aseptic surgery and the sterility of the implant, no antibiotic prophylaxis was used and no wounds became infected (Fig. 3A–E).

Bioelectrical characteristics

To determine the direct transmission electrical current (DTEC; micro-amp) and the tissue resistance to direct electrical current (TRDEC; micro-ohm) of the ITTCs, ITTC-PDS,

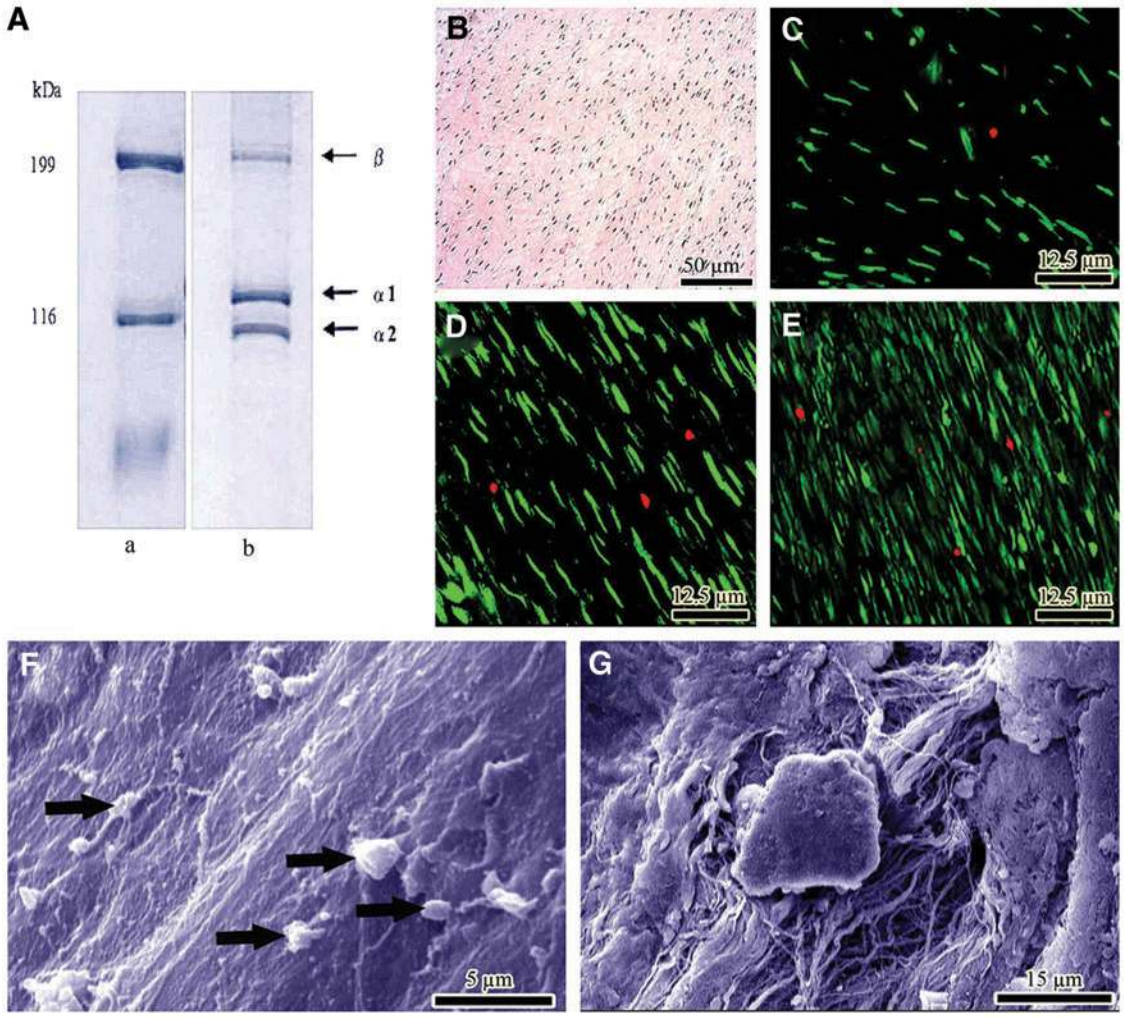

FIG. 2. *In vitro* tests. **(A)** SDS-PAGE images of type I collagen using 6% poly-acrylamide gel to examine the purification of collagen extracts. Lane a: molecular marker, lane b: bovine collagen. **(B)** Histologic section of the constructs after 20 days of cell culture. The proliferating fibroblasts are infiltrated to the implant and proliferated. **(C–E)** Cell viability was determined by live/dead cell assay using fluorescein diacetate (live) and propidium iodide (dead). **(C–E)** shows day 5, 10 and 20 after cell seeding. Almost all of the fibroblasts are green, indicating the cells are live. The lack of propidium iodide stained dead cells (red) supports the idea that normal rat fibroblasts have attached to the scaffold and that the majority of the cells are viable. **(F, G)** Surface and inside of the collagen implant after 20 days of cell seeding, respectively. The cells proliferated (arrows) and produced matrix. Color images available online at www.liebertpub.com/tea

ICTs and their NCTs, a bioelectrical measurement device (Digital Multi Pen Type Meter; Mastech) was used. The negative probe was placed on the medial aspect, and the positive probe on the lateral aspect of the tendon with its covering skin. DTEC and TRDEC were measured at weekly intervals from days 0 to 60 post injury.

Euthanasia

The animals were euthanized by intra-cardiac injection of a combination of 35 mg/kg Ketamine, 2 mg/kg Xylasin, and 1 mg/kg Acepromazine maleate (all from: Alfasan Co.) with 2 mg/kg gallamine triethiodide (Specia Co.).[6]

Sample collection

After euthanasia, both the injured ($n=30$ left tendons) and intact tendons ($n=30$ right tendons) of each experimental group were assessed for gross morphology. The injured and NCTs of each experimental group were randomly divided into two groups. In group 1, the tendons were subjected to tensile testing ($n=10$ left, $n=10$ right for each group) while the remaining tendons ($n=20$ left and $n=20$ right) were used as follows:

Each tendon ($n=20$ left and $n=20$ right) was longitudinally transected, and divided into three parts. The medial part was processed for light microscopy, the middle part for transmission electron microscopy (TEM), and the lateral part was used for determination of the biophysical characteristics.[36]

For the pilot animals, their injured ($n=5$ at each time point) and NCTs ($n=5$ at each time point) were investigated for gross morphologic and histopathologic analyses.

To simulate human Achilles tendon defects, we transected all the three strands of the rabbit Achilles tendon and anchored the tendon edges with modified Kessler core pattern;

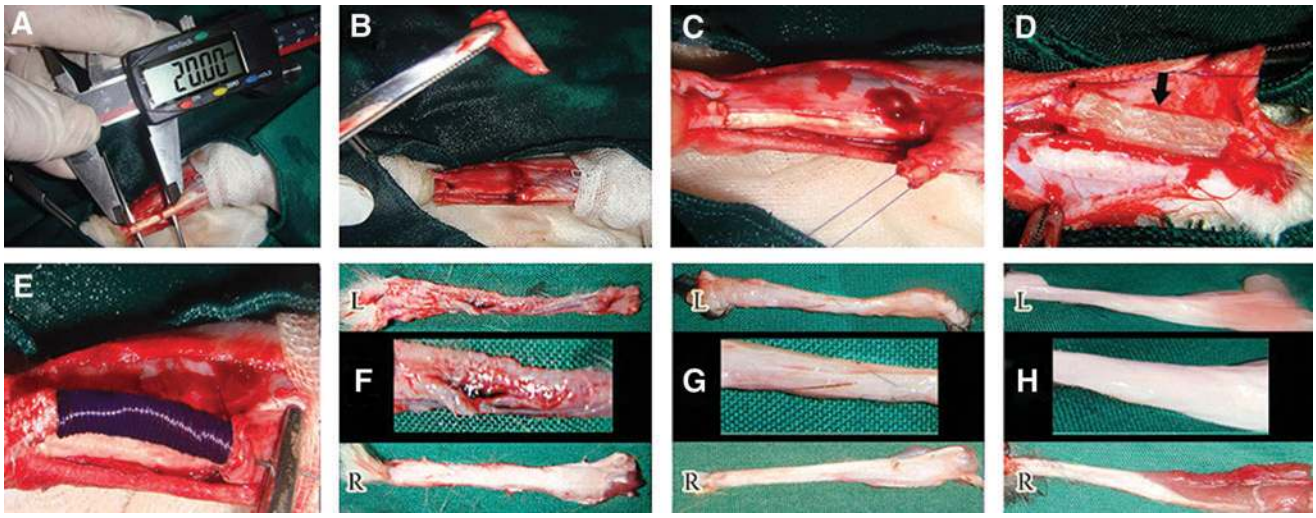

FIG. 3. Injury induction, surgical reconstruction and gross pathology. Two cm **(A)** of the Achilles apparatus discarded **(B)** and modified Kessler pattern was applied **(C)** in the remaining edges to maintain the gap at its 2 cm length. Collagen **(D)** and Collagen-polydioxanone sheath (PDS) **(E)** prosthesis were implanted in the defect area. At 60 days post injury (DPI), the injured control tendons (ICTs) had a marked hyperemia and a loose areolar connective tissue formed in the defect area **(F_L)**. Compared to their intact tendons **(F_R)**, these tendons showed lower diameter with diagnostic muscle atrophy and fibrosis **(F_L)**. At this stage the treated tendons with collagen **(G_L)** and collagen-PDS **(H_L)** prostheses, had transverse diameter comparable to their intact tendons **(G_R, H_R)**. These tendons were tendinous in nature and no hyperemia and peritendinous adhesions were seen **(G_L, H_L)**. Compared to their intact tendons **(G_R, H_R)** and their control tendons **(F_L)**, the amount of muscle fibrosis and atrophy was reduced in the collagen tendons (G_L vs. G_R) but these factors were more reduced in the collagen-PDS tendons (H_L vs. H_R). Color images available online at www.liebertpub.com/tea

therefore, the injured tendons regenerated as a single strand at 60 DPI. Therefore, the sections were only provided from one regenerated band. For the right tendons (NCTs), sections were provided from all the three strands but histologically, ultrastructurally and biophysically there were no differences between different strands.

Gross morphology

Each injured tendon ($n=30$ for each experimental group, $n=5$ for each pilot group) or NCT ($n=30$ for each experimental group, $n=5$ for each pilot group) was carefully evaluated. Hyperemia, peritendinous adhesions, general appearance, muscle atrophy, muscle fibrosis and tendon diameter were then measured and scored according to the previous methods.[6,7,37]

Light microscopy

After routine preparation of the samples (each experimental group: $n=20$ left, $n=20$ right; each pilot group: $n=5$ left, $n=5$ right),[6,7] they were stained using hematoxylin and eosin.[6] The samples were examined at light microscopy (Olympus). The photomicrographs were captured from the histologic fields and then transferred to the computer software (Adobe Photoshop CS-5) for digital analysis ($n^{\text{sample}}=20$, $n^{\text{histopathologic section}}=3$, $n^{\text{histopathologic field}}=5$, totally 300^L and 300^R histopathologic fields for each experimental group).[27] The number of tenoblasts, neutrophils, lymphocytes and macrophages of the tendon proper were counted ($\times 200$),[6,7] and the results were expressed as mean ± standard deviation (SD). The host graft interaction was followed in the histologic sections obtained from the pilot animals.

Transmission electron microscopy

The samples were fixed in cold 4% glutaraldehyde, dehydrated in graded ethanol, and embedded in epon resin 811 (TAAB Co.). Transverse sections of 70–80 nm thick (number of ultrathin section per sample = 3, number of samples in each experimental group = 20 left and 20 right) were prepared, and standard methods were employed for production of the ultramicrographs.[27] Number, diameter and density of the collagen fibrils of five different fields of the same magnification ($\times = 39000$) for each tissue section were measured and calculated by a computerized morphometric technique, using computer software (ImageJ, NIH).

In each group, the number of collagen fibrils and elastic fibers was counted in all the ultra-micrographs (magnification $\times 39000$), and the results were expressed as mean and SD. The transverse diameter of all the collagen fibrils of all the ultra-micrographs and the transverse diameter of 100 elastic fibers were measured and the results were expressed as mean and SD. For the density of the collagen fibrils, the area (nm^2) of the collagen fibrils in the ultra-micrographs was measured and reported as percentage of the total area (area of the ultramicrographs). Alignment and maturity of the collagen fibrils and elastic fibers were scored and analyzed as previously described.[6,7]

Biophysical characteristics

For percentage dry weight analysis, the injured tendons and their NCTs (for each experimental group: $n=20$ left and $n=20$ right) were weighed immediately after euthanasia, and then freeze-dried (Helosicc, Ink, Co.) to a constant dry weight, and the percentage dry weight was then calculated.[2,37] To determine water uptake capacity, each fully dehydrated

collagen implant was immersed in 0.9% isotonic saline solution, at 37°C for 48 h, to achieve its final wet weight. This weight was used as an index of wet weight of the implant, which was then freeze-dried. The fully dehydrated material was weighed and immersed in 0.9% isotonic saline solution at 37°C. From min 1 to min 480 after immersion, the implant was weighed at various time points. The water uptake capacity was calculated using the following equation: Index of water uptake = weight (dry)/time. The time refers to the point that the samples gained their maximum wet weight. To calculate their water delivery capacity, the fully hydrated samples were placed in a dry environment at 37°C, and left to evaporate their water content. From min 1 to min 3840 after air exposure, the samples were weighed at various time points. The index of delivery was calculated using the following equation: Index of water delivery = (Wwet)/Wdry $\times 100$/time. The time refers to the point that the samples lost their hydration and reach their dry weight. Analysis was performed based on the indices of normal tendons.

There were no significant differences between the wet weight of the samples immediately after euthanasia and the wet weight of the samples after saline immersion. Saline immersion had no role in protein depletion from the tissues.

Tensile testing

The method has been previously described.[2,6,7,27] Briefly, the distal end of the Achilles tendons ($n = 10$ left, $n = 10$ right in each experimental group) together with a portion of calcaneus were detached distally, and 3 cm of gastroc soleus muscle belly with its Achilles insertion were incised proximally. The tendons were mounted vertically, using a materials testing system (INSTRON® Tensile Testing Machine). We used a dual-cryogenic fixation assembly, holding the tendon securely at both ends. The gastroc soleus muscle and the tendinous insertion over the muscle were clamped in the upper jaw and the distal part of the tendon including tendon and the calcaneal part were clamped in the distal jaw. The flow of liquid nitrogen through a chamber within the cryoclamp was used to freeze the tendon in the clamp to prevent slippage of the tendons. Up to 1 mm of the tendon samples beyond the jaws were frozen. The freezing technology did not have any deleterious effect on the tensile testing results. A 30 mm portion of the tendon sample was adjusted between the jaws. Petroleum jelly was applied to the tested portions of the tendons to prevent dehydration and thermal injury. A heater was centered to prevent freezing of the portion to be tested, and two cardboard insulators protected the ice surface from melting. This setup ensured a sharp temperature gradient between the frozen ends of the tendon and the portion to be tested, which was undertaken at rabbit body temperature (37°C). The temperature of the portion to be tested was measured by a laser heat detector device in real time temperature prior and during tensile testing. Two thermocouples (one in each cryofixation assembly) closely monitored the degree of freezing. Care was taken to use the same condition for all the samples including treatment, control and intact tendons.

Each tendon was loaded by elongating it at a displacement rate of $10\,\text{mm}\cdot\text{s}^{-1}$ until a 50% decrease in load was detected. Load and crosshead displacement data were recorded at 1500 Hz, and the load-deformation and stress-strain curves were produced for each specimen using Test-Works 4 software (SUME Systems Corporation).

The load to failure is the maximum load that a material can withstand while being stretched or pulled before failing or breaking. Its unit is ''Newton'' often shortened to ''N''. Load at the yield point (SI unit: N) of a material is defined as the load at which a material begins to deform plastically. Prior to the yield point, the material will deform elastically and will return to its original length when the applied load is removed. Once the yield point is passed, part of the deformation will be permanent and nonreversible. In the force displacement curve, the maximum load is the higher registered load of the force displacement curve, and the yield is the point at which the curve ends its linear portion and commences a convexity towards the deformation axis. Stiffness is the rigidity of an object, that is, the extent to which it resists deformation in response to an applied force. The complementary concept is flexibility or pliability: the more flexible an object is, the less stiff it is. Stiffness was calculated by fitting a linear regression line to the load-deformation data from 30% to 90% of the maximal peak load on the deformation curve. The portion of the curve for defining stiffness should be after the toe region and before the yield point; it is measured in N/mm.

A strain is a normalized measure of deformation representing the displacement between particles in the body relative to a reference length. In this experiment, we measured the initial length between the two clamps before application of tension (L1) and at ultimate load (L2). The ultimate strain was measured as ([L2–L1] / L1) $\times 100$.

Ultimate tensile strength, often shortened to tensile strength or ultimate strength, is the maximum stress that a material can withstand while being stretched or pulled before failing or breaking. Maximum stress can be calculated as: Maximum stress = maximum load (load to failure) / cross sectional area of the sample. It is measured in N/mm^2. The cross section of the tendons was defined as an ellipse, the maximum and minimum diameters were measured, and the surface area was then calculated for each tendon. The large transverse diameter was measured from the medial to lateral part, and the small diameter was measured from the dorsal to plantar surface after the tendon was dissected.[6,7,27]

Elastic modulus, or modulus of elasticity, is the mathematical description of an object or substance's tendency to be deformed elastically (i.e., nonpermanently) when a force is applied to it. The elastic modulus of an object is defined as the slope of its stress–strain curve in the elastic deformation region; as such, a stiffer material will have a higher elastic modulus. Elastic modulus = Stress / Strian. Its unit is: N/mm^2.[6]

Statistical analysis

After application of the normal distribution test, the significant differences of the measured values within groups were statistically tested using paired-sample *t*-Test. The significant differences of the measured values between groups were tested using One Way ANOVA. The Kruskal-Wallis *H* Test was performed to analyze the scored data. Statistical analyses were performed using the computer software SPSS version 17 for windows (SPSS, Inc.). Differences of $p < 0.05$ were considered significant. For base scoring data, the median and range of the score was reported (median [min–max]).[7]

Results

Bioelectrical characteristics

At 7 DPI, the DTEC of the ICTs, ITTCs and ITTC-PDSs was significantly higher than 0 DPI ($p=0.001$). At 14 DPI, unlike ICTs, the DTEC of the ITTCs and ITTC-PDSs significantly increased, compared to 7 DPI ($p=0.001$ for both). At 20, 30 and 60 DPI, the DTEC of all the ICTs, ITTCs, ITTC-PDSs significantly decreased, compared to 14, 20 and 30 DPI, respectively ($p=0.001$ for all). The measured values for the ITTCs and ITTC-PDSs were significantly lower than those of the ICTs at 20, 30 and 60 DPI ($p=0.001$ for all). Although the DTEC of the ITTCs and ITTC-PDSs was significantly lower than the ICTs, the measured value of the DTEC of the ITTCs (2.77-fold) and ITTC-PDSs (2.49-fold) was significantly higher than those of 0 DPI ($p=0.001$ for both).

At 7 DPI, the TRDEC of the ITTCs (11.72-fold), ITTC-PDSs (8.11-fold) and ICTs (30.02-fold) was significantly lower ($p=0.001$ for all) than 0 DPI. At this stage, TRDEC of the ITTC-PDSs was significantly higher than that of the ITTCs ($p=0.001$) and ICTs ($p=0.001$). The measured value of the ITTCs was significantly higher than the TRDEC of the ICTs ($p=0.001$). Compared to 7 DPI, the TRDEC of the injured tendons of all groups at 14 DPI significantly decreased ($p<0.05$ for all). The TRDEC of the ITTC-PDSs was significantly higher than the TRDEC of the ITTCs, and the TRDEC of the ITTCs was significantly higher than the TRDEC of the ICTs at this stage ($p=0.001$ for all). Compared to 14 DPI, the TRDEC of the injured tendons of all groups significantly increased ($p=0.001$ for all), and the measured value for the ITTCs and ITTC-PDSs were significantly higher than the ICTs at 20 DPI ($p=0.001$ for both). The same pattern was seen at 30 DPI in these tendons. TRDEC of the ICTs, ITTCs, and ITTC-PDSs significantly increased at 60 DPI, compared to 30 DPI. At this stage, the TRDEC of the ITTC-PDSs was significantly higher than the TRDEC of the ITTCs, and the measured value for the ITTCs was significantly higher than the measured value of the ICTs ($p=0.001$ for all). Although the TRDEC of the ITTCs and ITTC-PDSs significantly increased at various time points after injury, they were still significantly lower than their normal ranges even at 60 DPI ($p=0.001$ for all), so that the ICTs, ITTCs and ITTC-PDSs gained 11.56%, 24.89% and 29.6% of their normal (0 DPI) TRDEC at this time (Fig. 4A, B).

Gross morphological findings

The ITTCs (3 [1–3]) and ITTC-PDS (2 [1–3]) showed significantly better scores for peritendinous adhesion compared to the ICTs (3 [2–3]; $p=0.049$, $p=0.021$, respectively). The ITTCs (2 [2–3]) and ITTC-PDS (2 [0–3]) also showed better scores for hyperemia compared to the ICTs (3 [2–3]; $p=0.035$, $p=0.003$, respectively). The ITTCs and ITTC-PDSs exhibited significantly better scores for muscle fibrosis (3 [1–3], 2 [0–3] vs. 3 [3–4], $p=0.042$, $p=0.001$ respectively), muscle atrophy (3 [0–3], 2 [1–3] vs. 3 [2–4], $p=0.049$, $p=0.017$ respectively), and general appearance of the injured tendons (2 [0–3], 2 [0–4] vs. 3 [1–4], $p=0.044$, $p=0.035$ respectively) compared to the ICTs. The transverse diameter of the ICTs in the injured area was significantly lower than the comparable area in their NCTs (1.89 ± 0.12 mm vs. 3.85 ± 0.32 mm, $p=0.001$). The transverse diameter was also significantly lower than the comparable area of the ITTCs (1.89 ± 0.12 mm vs. 4.12 ± 0.28 mm, $p=0.001$) and ITTC-PDSs (1.89 ± 0.12 mm vs. 4.19 ± 0.35 mm, $p=0.001$) (Fig. 3F–H).

Histologic findings

General report. After implantation of the prostheses, both the collagen and PDS scaffolds increased the inflammatory response compared with the control lesions. The inflammatory cells mainly consisted of neutrophils, lymphocytes and macrophages. The majority of the inflammatory cells during the initial stages of tendon healing were neutrophils which then declined during the fibroplasia and remodeling stages of tendon healing. The lymphocytes and macrophages were increased during the inflammatory and early remodeling stages (first 3 weeks after tendon injury) to decline thereafter. The inflammatory cells phagocytized some parts of the collagen implant during the inflammatory stage of tendon healing and the free spaces of the collagen implant were infiltrated by the newly regenerated connective tissue. When tendon healing progressed from the inflammatory to the fibroplasia stage, the remnants of the collagen implant, evident at histology, acted as micro scaffolds for the new tissue. The new tissue was then aligned along the direction of the collagen remnants during the fibroplasia and remodeling stages. No marked inflammatory reaction was seen around the collagen remnants, and they were gradually degraded or infiltrated by the healing tenoblasts during the course of the experiment. At 60 DPI, these processes resulted in the development of a new tendon which was aligned longitudinally between the gastrocnemius muscle and calcaneal tuberosity. The addition of PDS scaffold around the collagen implant reduced the development of peritendinous adhesion. It also increased the quality of the healing tissue in which the cells were more mature. The cells and collagen fibers showed a better alignment compared with those treated with the collagen implant alone. At that stage, the scaffold was partially degraded, and some remnants of the PDS scaffold were seen in the defect area around the new tendon. Unlike the treated lesions in which a new tendon was regenerated, the only regenerated tissue in the injured area was a loose areolar connective tissue which was filled with many immature vascular structures and immature collagen fibers. The fibers and cells were haphazardly distributed at different directions in the injured area and had invaded the peritendinous area and muscle fibers. The treated lesions also showed less muscle fibrosis and atrophy, and their muscle fibers were larger and denser compared with the control lesions (Figs. 5, 6).

Quantitative report (cell counting). After tendon injury and implantation of the prostheses, the number of tenoblasts, neutrophils, lymphocytes and macrophages significantly increased at 6 DPI, and were significantly higher in the treated lesions during the first 40 days following injury compared with the ICTs ($p=0.001$ for all). In comparison between the ITTCs and ITTC-PDSs, the PDS sheath significantly increased the number of neutrophils at 6 DPI, but there were no significant differences between the ITTCs and ITTC-PDSs at other stages of tendon healing. In all groups, the neutrophil counts was higher at 6 and 12 DPI and then significantly

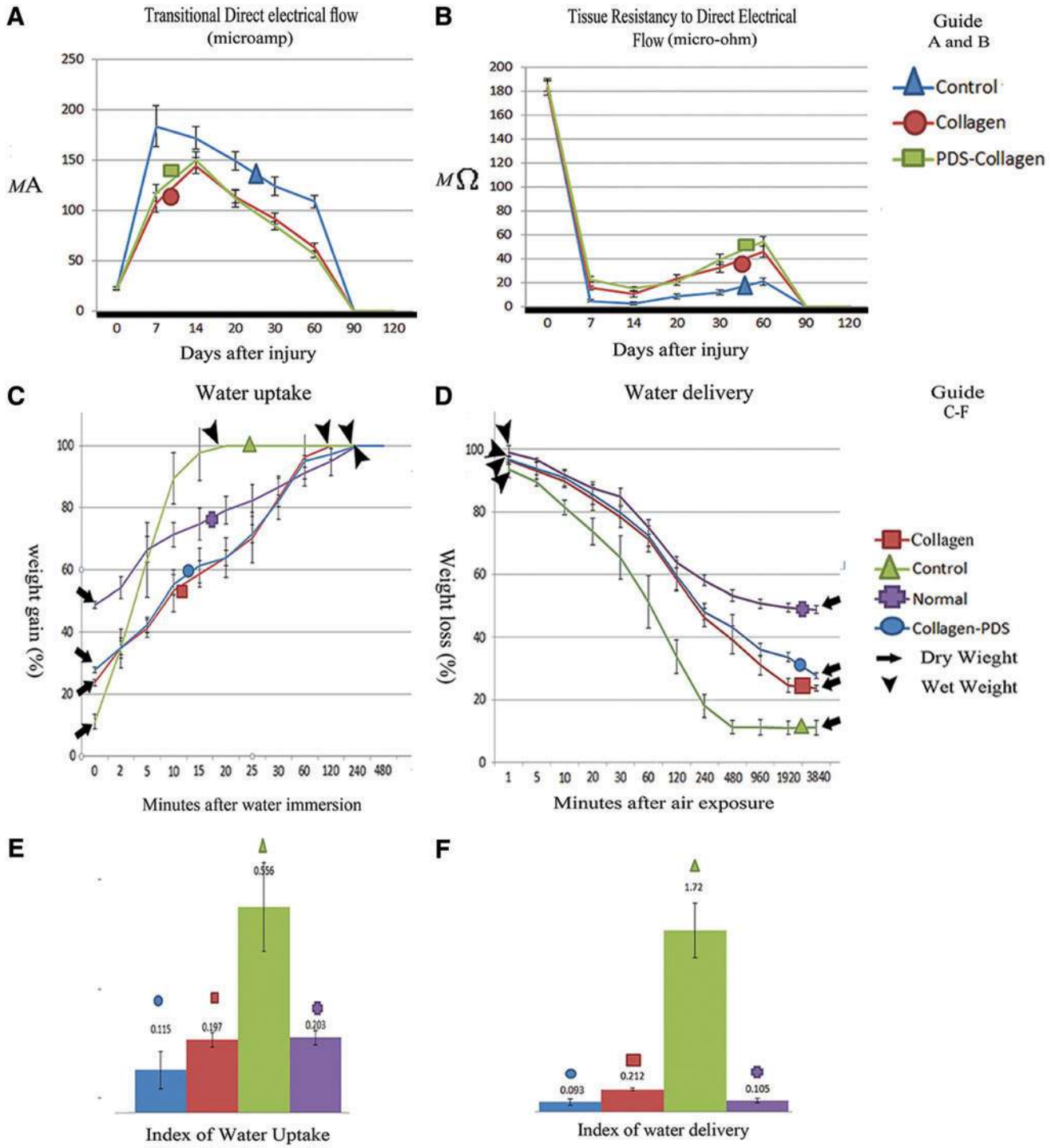

FIG. 4. Bioelectrical and biophysical characteristics of the injured tendons. The treated tendons with collagen and collagen-PDS prostheses had a significantly lower transitional direct electrical flow **(A)** ($p < 0.05$) and higher tissue resistancy to direct electrical flow **(B)** ($p < 0.05$) compared to the ICTs. However there were no significant differences between the treated groups ($p > 0.05$). The injured tendons treated with collagen and collagen-PDS prosthesis had a more similar diagrammatic pattern of water uptake **(C)** and water delivery **(D)** to the normal pattern at various time points, compared to the ICTs, so that, in the treated tendons the indices of water uptake **(E)** and delivery **(F)** were significantly lower than the ICTs and was close to normal value. Compared to the injured collagen tendons, the Collagen-PDS tendons showed significantly the lower indices of water uptake and water delivery ($p < 0.05$). Color images available online at www.liebertpub.com/tea

declined from 18 DPI to the end of the experiment ($p = 0.001$ for all). The lymphocytes and macrophages in the lesions of all groups declined from 24 DPI to the end of the experiment.

At 60 DPI, The ITTCs and ITTC-PDSs showed significantly higher number of tenoblasts compared with the ICTs ($p = 0.001$ for both), and the ITTC-PDSs showed a significantly higher number of lymphocytes and macrophages compared with the ICTs ($p = 0.001$ for both). There were no significant differences between the ITTCs and ITTC-PDSs at this stage ($p < 0.05$) (Fig. 7).

Ultrastructural findings (TEM)

General report. The collagen fibrils of the ICTs were small, unimodally distributed, and demonstrated low density. They showed a haphazard distribution pattern, so that in each section the collagen fibrils sectioned both transversely and longitudinally, and the cellular and fibrillar arrangement were not similar to normal tendinous structure (Fig. 8A–C). Immature tenoblasts were the most common cell types, and they had large, transparent cytoplasm with small proportion of nucleus to cytoplasm (Fig. 9A–C). The elastic fibers were mostly immature, and their orientation, organization and aggregation were far behind normal tendons (Fig. 8B). The collagen fibrils of the ITTCs (Fig. 8D–F) and ITTC-PDSs (Fig. 8G–I) were aligned unidirectionally so that they were sectioned almost longitudinally in longitudinal section. The collagen fibrils were distributed in a bimodal pattern, and their diameter and density had increased. All the microscopic field was filled with larger collagen fibrils, and the cells laid in the directions of the collagen fibrils (Fig. 9D, E). The elastic fibers were larger, and showed a more advanced alignment and maturation pattern. Few remnants of the collagen implant were present in the injured area, so that the newly regenerated collagen fibrils surrounded them and aligned along their orientation (Fig. 9F).

On the other hand, the collagen fibrils of the NCTs (Fig. 8J–L) were highly aligned in a unidirectional pattern, and very scanty cigar-shape tenocytes and, rarely, fewer mature tenoblasts were laid in the direction of the collagen fibrils. The elastic fibers were rare but highly mature, and well organized. The collagen fibrils were distributed in a multimodal pattern with marked density and maturity. The large collagen fibrils were surrounded by the smaller collagen fibrils and provided a unique organizational pattern, typical of normal tendinous tissue.

Quantitative report. ITTCs and ITTC-PDS showed significantly higher rate of collagen fibrillogenesis compared to ICTs (590.08 ± 28.81, 652.77 ± 24.28 vs. 350.26 ± 21.71, $p = 0.001$, $p = 0.001$ respectively) (Table 1). The ITTC-PDSs showed higher fibrillogenesis than the ITTCs ($p = 0.046$). The collagen fibrils of the ICTs were in the range of 0–64 nm, and those of the ITTCs and ITTC-PDSs differentiated into two different categories of 0–64 and 65–102 nm. The number of collagen fibrils in the range of 65–102 nm in the ITTC-PDSs was significantly higher than the ITTCs (75.27 ± 7.65 vs. 48.95 ± 8, $p = 0.001$). Although the collagen fibrils of the treated groups differentiated into two different ranges of diameter, their NCTs showed five different ranges of 0–64, 65–102, 103–153, 154–256 and 257–307 nm collagen fibrils.

The ITTCs and ITTC-PDSs showed significantly higher diameter of the collagen fibrils compared to the ICTs ($p = 0.001$ for all). The mean total diameter of the collagen fibrils of the ITTC-PDSs was significantly higher than the ITTCs (58.73 ± 2.75 nm vs. 47.96 ± 1.6 nm, $p = 0.001$), but was significantly lower than their NCTs (58.73 ± 2.75 nm vs. 110.16 ± 9.76 nm, $p = 0.001$). The density of the collagen fibrils of the ITTCs and ITTC-PDSs was significantly higher than the ICTs ($66.23\% \pm 5.28\%$, $72.24\% \pm 5.01\%$ vs. $47.15\% \pm 4.17\%$, $p = 0.001$ for both), but was significantly lower than their NCTs ($p = 0.001$ for both). ITTCs and ITTC-PDSs showed higher number and diameter of elastic fibers compared to the ICTs ($p = 0.001$). In the ITTCs and ITTC-PDSs, the transverse diameter of the immature fibroblasts and fibrocytes was significantly lower than the ICTs ($p < 0.05$). $29.21\% \pm 3.02\%$ of the ITTC-PDSs, $20.06\% \pm 4.85\%$ of the ITTCs, $4.19\% \pm 1.02\%$ of the ICTs and $97.81\% \pm 2.77\%$ of the NCTs were mature tenoblasts or tenocytes. The differences between groups were statistically significant ($p = 0.001$ for all).

FIG. 5. Histopathologic evaluations: Host graft interaction and earlier stages of tendon healing. **(A–I)** Injured treated tendon treated with collagen implant (ITTC). **(J–L)** ICT. **(A)** At 6 DPI the collagen implant absorbed the inflammatory cells in its structure so that a demarcation line could be seen between the inflammation (I) and the collagen remnant (C.R). **(B–D)** At 12 DPI the inflammatory cells mainly consisted of neutrophils and macrophages infiltrate throughout the collagen implant and phagocytized some areas of the collagen implant so that the C.R and the inflammation can be seen in the histologic field. **(E)** At 18 DPI, some parts of the collagen implant are completely degraded by the inflammatory cells and the newly regenerated connective tissue regenerated between the C.R. At this stage some parts of the collagen implant are phagocytizing by the inflammation (I) and the C.R. which is not affected by the inflammation (I) is preserved. At 24 DPI **(F)**, the inflammation was subsided and the fibroplasia stage of tendon healing is in progress. Several C.R are still present in the defect area but the free spaces between them are completely filled by the new tendon (N.T). At 30 DPI, the proportion of the C.R. is reduced and the N.T is predominant at this stage **(G)**. Note that the C.R. are now infiltrated by the healing tenoblasts and the C.R. acted as a micro-scaffold for the N.T, so that is aligned the N.T along its longitudinal direction. **(H)** At 40 DPI, The proportion of the C.R. is greatly decreased as compared with **(G)** No inflammatory cells can be seen around these C.Rs. At 60 DPI **(I)** most of the collagen implant is absorbed and the majority of the new tendon is belonged to the newly regenerated tendon (N.T). This tendon is aligned and its histologic characteristics give this concept that the healing tissue is in the remodeling phase of tendon healing. **(J–L)** ICT at 12, 30 and 60 DPI, respectively. Note that the amount of inflammatory cells are lower than the ITTC. The tissue is not organized and its histologic characteristics is almost similar to loos areolar connective tissue which mimic the subcutaneous fascia, even after 60 days **(L–O)** 12 DPI. The collagen implant greatly increased the inflammation in the ITTC at 12 DPI **(N)**, as compared with the ICT **(M)** The collagen-PDS implant increased the inflammation in the injured treated tendons more than M and N. The majority of the inflammatory cells in **(M–O)** are belonged to the neutrophils which have phagocytic activity. Color staining: H&E. Color images available online at www.liebertpub.com/tea

Compared to the ICTs (3.5 [3–4]), the ITTCs (2.5 [1–3]) and ITTC-PDSs (2 [0–3]) showed significantly better scores for alignment of the collagen fibrils ($p = 0.049$, $p = 0.012$, respectively). Also, ITTCs 3 [3–3.5] and ITTC-PDSs (3 [2–3]) showed significantly better scores in collagen maturity compared to ICTs (4 [4–4]), $p = 0.042$, $p = 0.027$, respectively. Compared to the ICTs (3 [3–3]), the ITTCs (2 [1–2]) and ITTC-PDSs (1 [1–2]) showed significantly better scores for maturity of the elastic fibers ($p = 0.035$, $p = 0.001$, respectively).

Biophysical characteristics

ITTC-PDSs showed significantly higher dry matter content compared to the ITTCs (27.76% ± 0.93% vs. 23.67% ± 1.35%; $p = 0.001$) and ICTs (27.76% ± 0.93% vs. 11.12%; $p = 0.001$). In addition, ITTCs had significantly higher dry matter content compared to the ICTs ($p = 0.001$). The dried ICTs gained their maximum wet weight 20 min after water immersion (MPWI). Compared to the ICTs, the dried ITTCs,

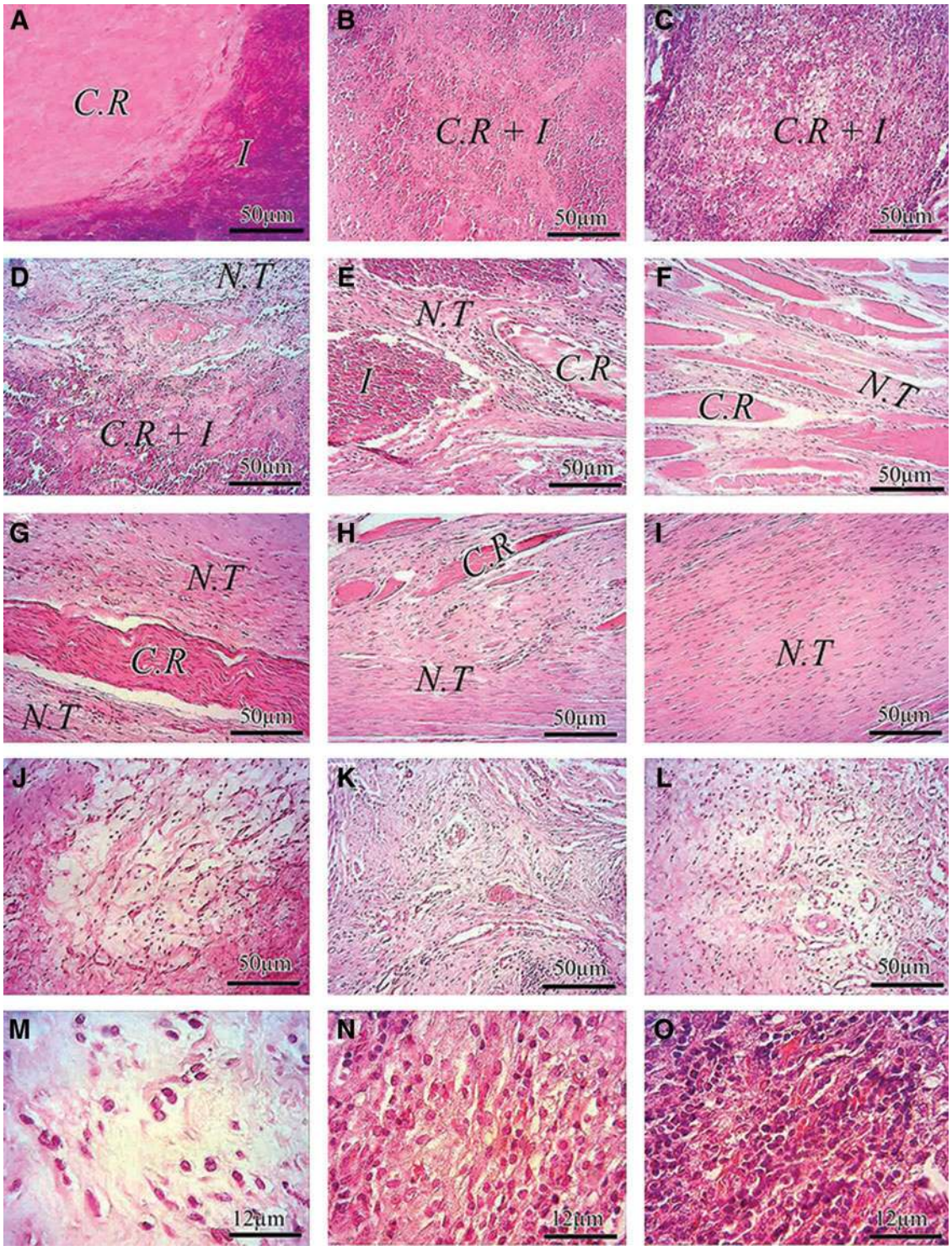

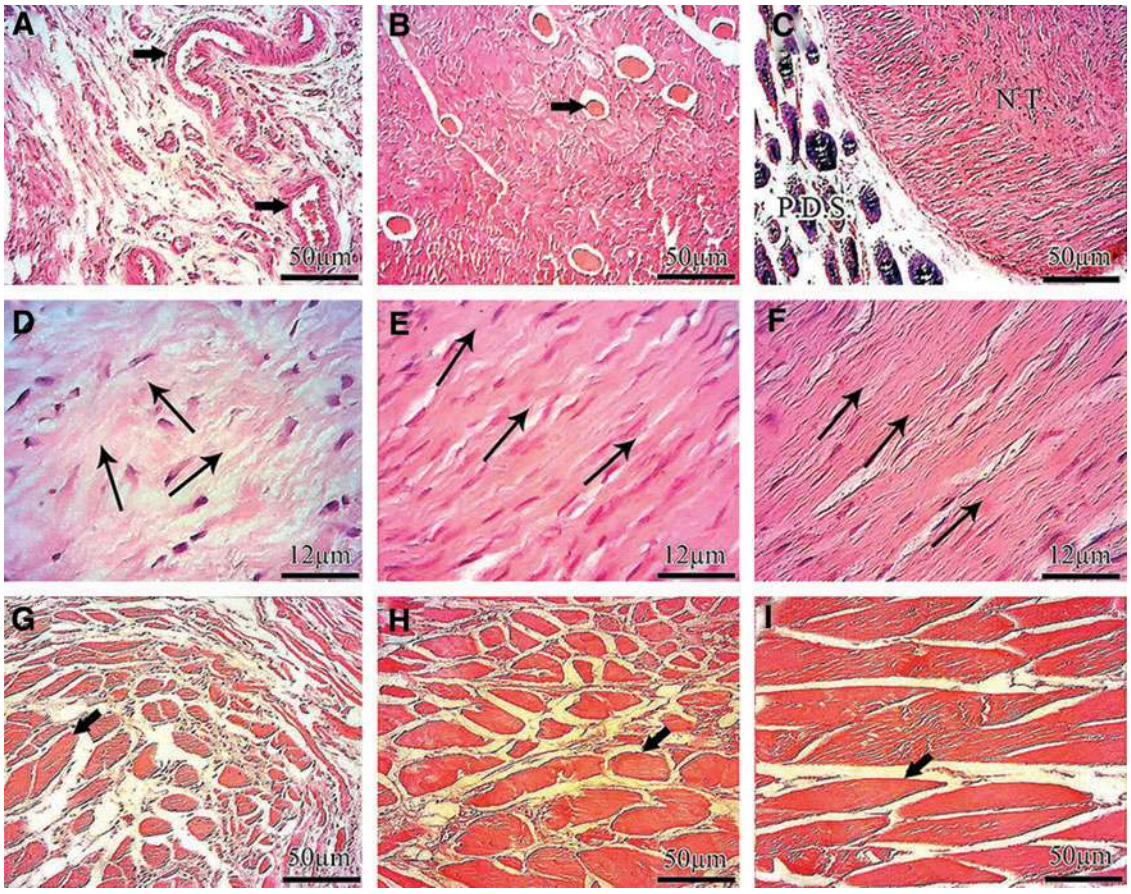

FIG. 6. Histopathologic characteristics of the injured tendons at 60 DPI. **(A–I)** 60 DPI. **(A–C)** and **(G–I)**: transverse sections. **(D–F)** longitudinal sections. **(A)** ICT. **(B)** ITTC. **(C)** injured treated tendon with collagen-polydioxanon implant (ITTC-PDS). At 60 DPI, the newly regenerated tissue filled the defect area of the ICT, was amorphous in nature and several vascularity (Arrow) with poor organization of the collagen fibers and cell alignment were evident in the histologic field. This tissue had low density of the collagen fibers and there was no evidence regarding formation of the new tendon. Unlike ICT **(A)** the new tendon was formed in the defect area of the ITTC **(B)** and some collagen remnant (Arrow) were observable through the new tendon however the majority of the defect area was belonged to the new tendon not the collagen remnant. The proportion of the collagen remnants were lower in the ITTC-PDSs **(C)** as compared with the ITTC and the remnants of the PDS were present around the new tendon. The new tendon was formed though this PDS sheath. **(D)**: at 60 DPI, the collagen fibers and the cells were oriented randomly. The arrows show the cellular and fiber directions. Note that more than two major direction could be seen in the histologic section **(D)** The cells are immature mainly consisted of lymphocytes and immature tenoblasts **(D)** At this stage the cellular structures of the ITTC **(E)** and ITTC-PDS **(F)** laid in only one direction (arrows show the direction) and the density of the collagen fibers are higher and the cells are more mature, mainly consisted of mature tenoblasts and tenocytes as compared with the ICT **(D)** At 60 DPI, the gastroc-soleus muscle of the ICT was atrophied and the fibrous connective tissue filled the free spaces between the atrophied muscle fibers **(G)** The ITTC **(H)** and ITTC-PDS **(I)** showed less muscle atrophy and fibrosis compared to the ICT. The muscle fibers are indicated by arrows **(G-I)** Color staining: hematoxylin and eosin. Color images available online at www.liebertpub.com/tea

ITTC-PDS and NCTs gained their wet weight at 120 (6-fold), 240 (12-fold) and 480 (24-fold) MPWI. The NCTs, ITTCs and ITTC-PDSs also showed significantly lower indices of water uptake compared to the ICTs (0.203 ± 0.06^{NCTs} vs. 0.197 ± 0.05^{ITTC} vs. $0.115 \pm 0.06^{ITTC\text{-}PDS}$ vs. 0.556 ± 0.12^{ICTs}, $p = 0.001$). The difference between ITTCs and ITTC-PDSs was not statistically significant ($p = 0.051$).

By air exposure of the fully hydrated samples, the wet weight of the ITTCs and ITTC-PDSs gradually diminished so that they reached their dry weight at 3840 min post air exposure (MPAE). However, the ICTs reached their dry weight at 960 MPAE, so that both of the treated tendons lost their wet weight later than the ICTs (4-folds). Compared to the ITTCs and ITTC-PDSs, the NCTs reached their dry weight at 7680 MPAE and they lost their wet weight later than treated tendons (2-fold) and control tendons (8-fold). The ICTs had a significantly higher index of water delivery compared to the NCTs, ITTCs, and ITTC-PDSs (1.72 ± 0.21 vs. 0.105 ± 0.01, 0.212 ± 0.03, 0.093 ± 0.01, $p = 0.001$), and the indices of the treated tendons were more comparable to normal tendons. However, compared to the ITTCs, the index of water delivery of the ITTC-PDSs was closer to NCTs (Fig. 4C–F).

Biomechanical findings

Treatment with collagen and collagen-PDS implants significantly increased the load to failure, load to yield point, stiffness, maximum and yield stress and modulus of

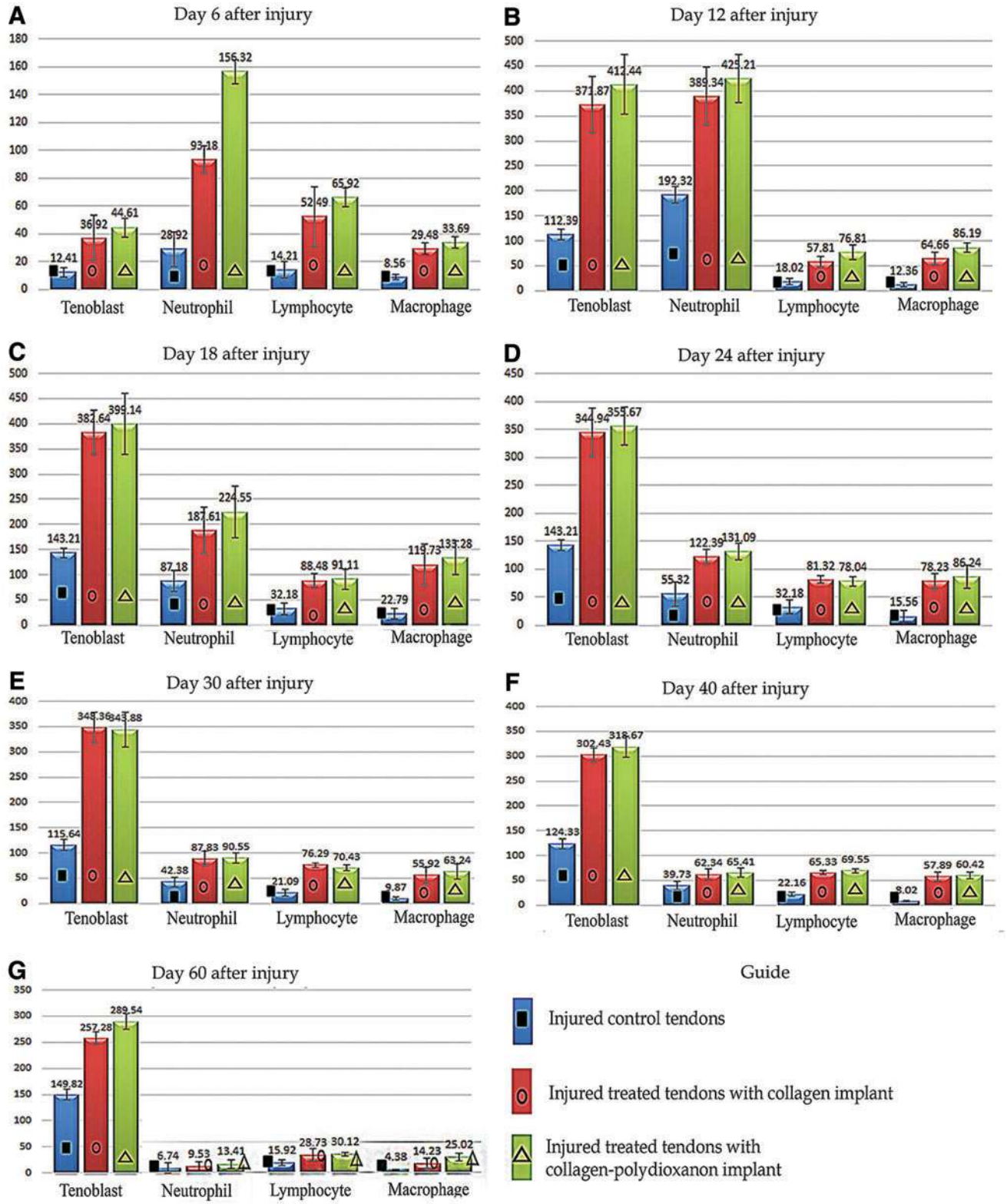

FIG. 7. Quantitative histopathologic results at different stages of tendon healing. Number of tenoblasts, neutrophils, macrophages and lymphocytes in the injured area of the treated and control groups at different time points **(A–G)**. Number of samples in each group: (1) experimental groups at 60 DPI = 20; (2) pilot groups at 6 to 40 DPI = each time point had five samples. One way ANOVA with its subsequent *post hoc* Tukey test was used to statistically analyze the measured values. The results were expressed as mean ± standard deviation (SD) and differences were considered statistically significant at $p < 0.05$. Cell counting was performed in triplicate and the average was calculated. Color images available online at www .liebertpub.com/tea

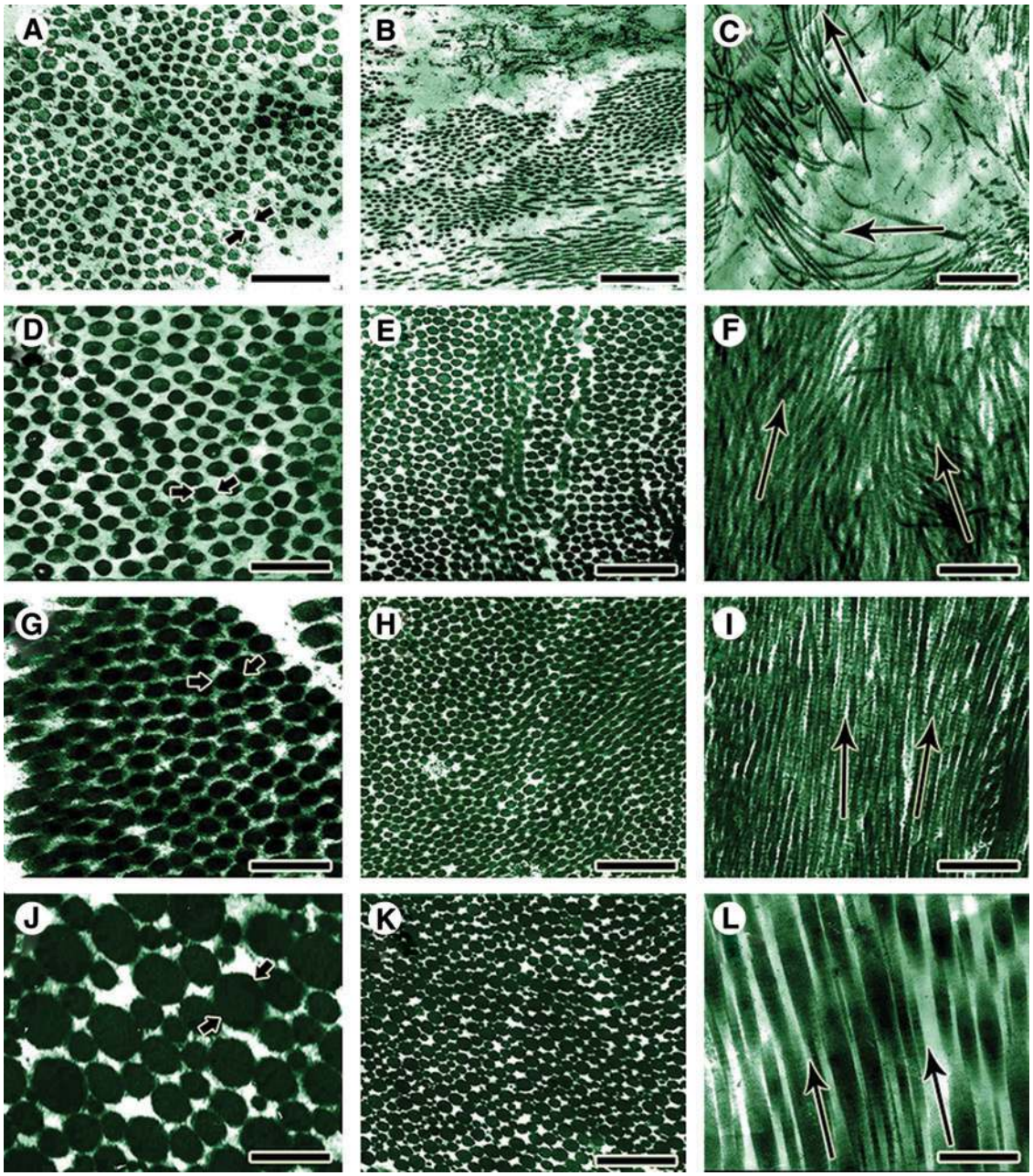

FIG. 8. Ultra structure of the injured and normal tendons (Transmission electron microscopy). In the ICTs, the transvers diameter of the newly regenerated collagen fibrils **(A**, between arrows**)** was low and they had uni-modal distribution pattern **(A, B)**. At longitudinal section these collagen fibrils, were laid in multidirectional pattern (**C**, arrows) with no marked orientation and compactness **(C)** In the treated tendons with collagen **(D–F)** and collagen-PDS **(G–I)** prostheses, the newly regenerated collagen fibrils had bimodal distribution pattern and their diameter (**D** and **G**, between arrows) and density was significantly higher than the ICTs. At longitudinal **(F, I)** and transverse **(E, H)** section, these fibrils were oriented in only one direction (**F** and **I**, Arrows show the orientation of the collagen fibrils) and they were compact. Although the treated collagen-PDS tendon had better morphological characteristics compared to the treated collagen tendons, however the differences were not significant mainly ($p > 0.05$). In normal uninjured tendons **(J–L)**, the collagen fibrils had the same characteristics as the treated tendons but they were distributed in multimodal pattern so that more than two different category of fibril diameter (**J**, a large collagen fibrils is indicated by the arrows) were present in these tendons. The normal collagen fibrils are highly aligned so that in a longitudinal section **(L)** these fibrils are laid in only one direction. The arrows (**L**) shows the direction of these fibrils. Scale bar **A, D, G, J** = 171 nm, **B, E, H, K** = 495 nm, **C, F, I, L** = 742 nm. Color images available online at www.liebertpub.com/tea

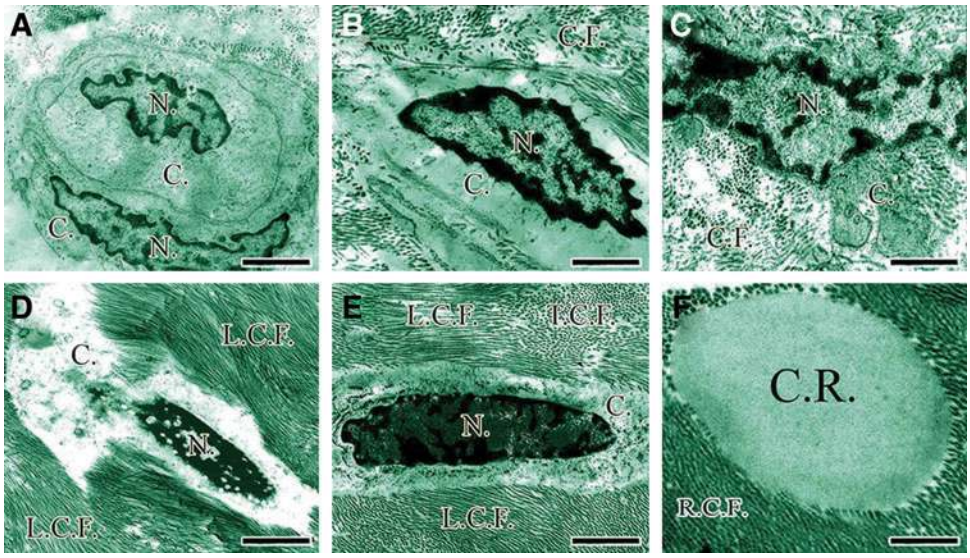

FIG. 9. Differentiation of the tendon cells at ultra-structure level. A newly divided immature mesenchymal cells with the lower proportion of the nuclei (N.)/cytoplasm (C.) so that most of the cell's environment is cytoplasm (C.) **(A)** These cells can be found in the newly regenerated tissue because they result from the new duplication **(A)** As the time goes on, these cells become activated so that their nucleus (N.) is elongated **(B)** and rough endoplasmic reticulum, Golgi bodies and other cytoplasmic organelles develop and the pockets of collagen molecules are seen in their cytoplasm (**C**, C.). Over time, the proportion of nuclei (N.)/cytoplasm (C.) increases and when the mature fibroblasts **(D)** are in the transitional stage from the mature fibroblasts to fibrocytes **(E)**, their size and activity of their cytoplasm (C.) decreases and the shape of these cells changes from the oval shape to cigar shape (**D** vs. **E**). In **(D, E)** the longitudinally sectioned collagen fibrils (L.C.F.) and the transversely sectioned collagen fibrils (T.C.F.) are shown by the letters (L.C.F. vs. T.S.C.). As it has shown in **(F)**, the remnant of the collagen implant is present at the center of the figure and the newly regenerated collagen fibrils growth in the direction of this remnant, so that at transvers sectioning, both the collagen remnant (C.R.) and the newly regenerated collagen fibrils (R.C.F.) sectioned transversely in the same manner **(F)**. Scale bar **A** = 1800 nm, **B** = 750 nm, **C** = 800 nm, **D** = 1760 nm, **E** = 1240 nm, **F** = 800 nm. Color images available online at www.liebertpub.com/tea

elasticity of the ITTCs and ITTC-PDSs, at 60 DPI, compared with the ICTs ($p = 0.001$ for all). At this stage, treatment with collagen-PDS implant also significantly increased the load to failure and load to yield point compared with the ITTCs ($p = 0.001$ for both). The biomechanical properties of the treated lesions were still significantly inferior compared to those of their NCTs at 60 DPI ($p = 0.001$ for all). The ICTs, ITTCs and ITTC-PDSs showed 2.81%, 15.1% and 21.2% of the load to failure, 19.23%, 46.54% and 50.15% of the maximum stress, and 6.25%, 21.61% and 28.56% of the modulus of elasticity of their NCTs at this stage (Fig. 10).

Discussion

Unassisted healing in the control animals failed to produce a new tendon in the large Achilles tendon defect. On the other hand, implantation of the prostheses resulted in regeneration of a new tendinous tissue. The results of this preliminary study demonstrate that the treatment strategy was able to significantly reduce the tendon adhesions and muscle atrophy and increase the physical and morphological performance of the new tendon compared with the control lesions.

Unlike the unassisted healing in the control tendon, the implant was initially able to accelerate the inflammation in the defect area for a longer period, because the DTEC of the ITTCs and ITTC-PDSs elevated up to 14 DPI. After tendon injury, exaggerated inflammation is harmful, but inflammation is necessary to initiate an appropriate healing response.[2,24] At this phase, the inflammatory cells infiltrate into the defect area and produce swelling in the injured area.[25,27] The inflammatory cells and matrix metalloproteinases start to degrade the injured tissue to facilitate fibroplasia and remodeling phases of tendon healing. Edema, inflammatory cell infiltration and lack of proper organization at earlier stages of healing normally result in swelling and lower dry matter content of the injured area.[24] Our results suggest that, by decreasing the dry matter content and increasing the water content of the injured tissue, electrical ions could circulate into the injured area faster than in normal tissue.[38] Our histologic results confirmed the above results, and demonstrated that, although inflammation is increased by the presence of the prostheses, the inflammatory cells declined after the inflammatory phase of tendon healing, and no marked inflammation was seen during fibroplasia and remodeling stages of tendon healing in the treated lesions. Severe and prolonged inflammatory reaction is not beneficial in tendon healing. By modulation of inflammation, the healing response could be improved.[2,6,27,37]

It is possible that the remaining solvents of the collagen implant that had been added to the collagen solution during preparation of the collagen implant initiated inflammation at the inflammatory stage of tendon healing. However, we examined the cytocompatibility of the implants, and they were highly cytocompatible. The other possibility is that the implant was infected and, given the presence of infection, the inflammatory cells invaded the implant. We showed that the implants were sterile. Also, we tested the endotoxin content,

Table 1. Ultrastructural Findings of the Injured Treated (Collagen and Collagen-PDS), Injured Control and Intact Tendons, 60 Days Post Injury and Surgical Reconstruction (Quantitative Assessments Obtained from Transmission Electron Microscopy)

		60 DPI Control (1) (no implant)	*60 DPI Collagen (2)*	*60 DPI Collagen-PDS (3)*	*Normal (4)*	p *value 1 vs. 2*	p *value 1 vs. 3*	p *value 1 vs. 4*	p *value 2 vs. 3*	p *value 2 vs. 4*	p *value 3 vs. 4*
Number of collagen fibrils based on their category and totally in ultramicrographs in the same magnification (39000)	Fibrils (0–64 nm) (N)	350.26 ± 21.71	549.8 ± 26	597.18 ± 18.78	56.78 ± 5.39	0.001	0.001	0.001	0.081	0.001	0.001
	Fibrils (65–102 nm) (N)	0	48.95 ± 8	75.27 ± 7.65	18.39 ± 2.11	–	–	–	0.001	0.001	0.001
	Fibrils (103–153 nm) (N)	0	0	0	17.68 ± 3.53	–	–	–	–	–	–
	Fibrils (154–256 nm) (N)	0	0	0	22.38 ± 3.88	–	–	–	–	–	–
	Fibrils (256–307 nm) (N)	0	0	0	3.34 ± 0.89	–	–	–	–	–	–
	Total (N)	350.26 ± 21.71	590.08 ± 28.81	652.77 ± 24.28	118.24 ± 2.85	0.001	0.001	0.001	0.046	0.001	0.001
Diameter of collagen fibrils based on their category and totally in ultramicrographs (nm)	Fibrils (0–64 nm) (D)	28.72 ± 2.46	45.28 ± 5.19	54.45 ± 2.03	48.79 ± 2.42	0.001	0.001	0.001	0.019	0.572	0.027
	Fibrils (65–102 nm) (D)	0	72.96 ± 4.68	86.66 ± 4.23	100.45 ± 5.39	–	–	–	0.001	0.001	0.001
	Fibrils (103–153 nm) (D)	0	0	0	149.79 ± 10.89	–	–	–	–	–	–
	Fibrils (154–256 nm) (D)	0	0	0	238.78 ± 4.21	–	–	–	–	–	–
	Fibrils (256–307 nm) (D)	0	0	0	276.48 ± 21.33	–	–	–	–	–	–
	Total (D)	28.72 ± 2.46	47.96 ± 1.6	58.73 ± 2.75	110.16 ± 9.76	0.001	0.001	0.001	0.001	0.001	0.001
Area of the fibrils/area of the ultramicrographs	Fibril density (%)	47.15 ± 4.17	66.23 ± 5.28	72.24 ± 5.01	89.47 ± 5.59	0.001	0.001	0.001	0.495	0.001	0.001
Number of elastic fibers in ultramicrographs	Elastic fiber (N)	2.33 ± 0.66	8.93 ± 1.46	6.8 ± 0.93	9.56 ± 1.29	0.001	0.001	0.001	0.781	0.594	0.001
Diameter of the cells and elastic fibers (nm)	Immature fibroblast (D)	8429.48 ± 557.24	6764.45 ± 345.7	6456.23 ± 300.79	–	0.001	0.001	–	0.809	–	–
	Mature fibroblast (D)	3787.39 ± 146.91	3582.81 ± 148.18	3352.38 ± 158.55	–	0.778	0.049	–	0.232	–	–
	Fibrocyte (D)	1848.42 ± 74.01	1673.26 ± 98.62	1521.9 ± 61.62	985.49 ± 54.82	0.049	0.001	0.001	0.178	0.001	0.001
	Elastic fiber (D)	56.26 ± 7.58	113.03 ± 16.94	139.23 ± 9.63	279.27 ± 14.28	0.001	0.001	0.052	0.001	0.001	0.001

Ultramicrographs: $n = 5$. Ultrathin sections: $n = 3$. Tendon samples: $n = 20$. Total picture for each group: $n = 300$. The significant differences of the measured values between multiple groups were tested using One Way ANOVA with *post hoc* Tukey test. Significant differences were determined at confidence interval of 95% and $p < 0.05$.

DPI, days post injury; PDS, polydioxanone sheath; D, diameter; N, number.

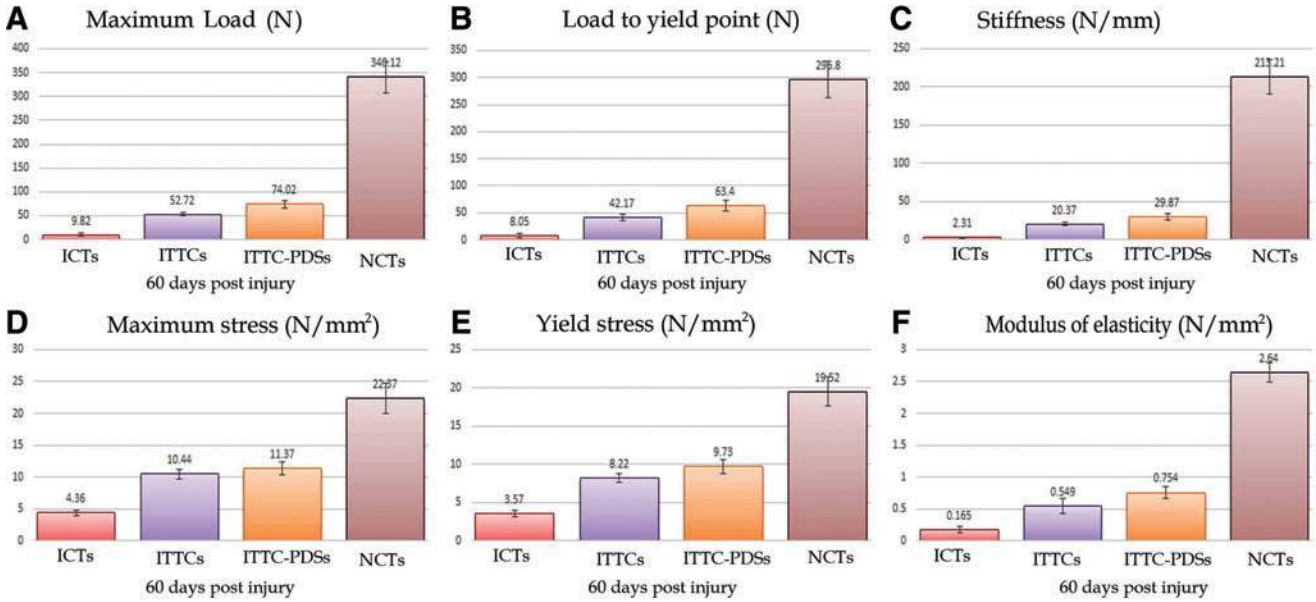

FIG. 10. Biomechanical characteristics of the injured treated, control and their normal contralateral tendons (NCTs) after 60 days of tendon injury **(A–F)**. The ITTCs ($n=10$) and those treated with collagen-PDS implant (ITTC-PDSs; $n=10$) showed significantly the higher load to failure, load to yield point, stiffness, maximum and yield stress and modulus of elasticity as compared with those in the ICTs ($n=10$) ($p=0.001$ for all). However at this stage (after 60 days), the treated lesions had significantly lower biomechanical properties as compared with those in their NCTs ($p=0.001$ for all). The results are expressed as mean ± SD. Color images available online at www.liebertpub.com/tea

and showed that the implants had minimum amounts of endotoxins. It is possible that the molecules of the scaffolds in a large volume have some immunogenic activity and can attract inflammatory cells, thus motivating an inflammatory response. This effect was possibly because of the biodegradability and biocompatibility of the implants, which was confirmed at histology.[9,19,39,40]

The covering PDS scaffold did not exert deleterious effects on inflammation, and its combination with the collagen implant did not increase markedly the severity of inflammation. Probably, this characteristic resulted from the absorption of the PDS scaffold. The mechanism of degradation and absorption of the collagen implants is related to their phagocytosis by the inflammatory cells, whereas absorption of the PDS scaffolds occurs by hydrolysis.[41]

Our results demonstrated that the collagen implant not only increases the number of the inflammatory cells, but it also has a similar role in increasing the number of tenoblasts. Collagen molecules are chemo-attractive for fibroblasts.[42] Probably, this characteristic of the collagen molecules attracted fibroblasts to the implant, and, given the highly aligned organization of the collagen fibers of the implant, the migrated fibroblasts aligned and proliferate along the direction of these fibers. Using a disorganized scaffold is more likely to produce a highly disorganized tissue, delay production of useful matrix, and prevent uniform remodeling.[43] In tendon healing, appropriate organization results in improved structural organization and physical performance of the injured tendon.[19,24]

At macro-, micro- and ultra-structural level, most of the implants were degraded at 60 DPI, and the majority of the tissue placed in the defect area belonged to the new tendon, not the implant. This is one of the merits of the implant. These remnants of the collagen scaffolds probably acted as scaffolds, and they had a role in aligning the newly regenerated tenoblasts, collagen fibrils and fibers along their longitudinal direction. Our histologic results confirmed that the direction of collagen remnants was in accordance with the normal Achilles tendon direction between from the gastroc-soleus muscle to the calcaneus. After simple tendon transection, the preserved collagen fibrils acted as scaffolds for the newly regenerated collagen fibrils *in vivo*.[26,44]

The ITTCs and ITTC-PDSs showed higher number of mature tenoblasts compared to the ICTs. The cellular structures in the treated lesions were metabolically active, and they produced large amounts of collagen and glycosaminoglycans around themselves. Higher number and greater diameter and density of the collagen fibrils regenerated in the injured area of the ITTCs and ITTC-PDSs at 60 DPI demonstrated that these tendons were dense, and their biophysical and bioelectrical characteristics were significantly superior to those of ICTs. Number, diameter and density of the collagen fibrils show evidence of a statistically significant association with the biomechanical and biophysical properties of the injured tendons *in vivo*.[2,36] In addition, greater collagen fibril deposition and differentiation show evidence of a statistically significant association with the higher dry matter content and the improved indices of water uptake and water delivery of the ITTCs and ITTC-PDSs compared to the ICTs. The lower amount of DTEC and higher amount of TRDEC in the ITTCs and ITTC-PDSs compared to the ICTs, at 60 DPI, also support the above biophysical and structural changes. Perhaps, the increase in the dry matter content or decrease in hydration of the injured area, together with improved alignment, result in greater compactness of the collagen fibrils and fibers; this would be the main reason why

less electrical ions are transmitted through the healing tissue compared to the inflammatory phase observed in the first 14 DPI. In such situation, TRDEC increases.

In the present study, there is evidence of a negative association between changes of the DTEC and TRDEC in the injured area. Therefore, if one of them increases, the other will decreases. Others have shown that progress in the healing phases modulates the bioelectrical characteristics of the newly regenerated tissue.[45–47] When a tissue is damaged, its bioelectrical characteristics change, so that the electrical currents diminish as healing progresses, and the normal values is reestablished once healing is completed.[38,47]

A major role of the collagen implant and its covering PDS sheath was to conduct the migrated fibroblasts in the longitudinal axis of the implant; we clarified this as a tenoconductive characteristic. This longitudinal axis was along the normal anatomical direction of the tendon-muscle unit. Thus, the migrating fibroblasts mostly proliferated throughout the implant, and did not invade the peripheral tissues and gastrocnemius muscle, resulting in lower peritendinous adhesion and muscle fibrosis in the ITTCs and ITTC-PDSs. These animals may have exhibited better weight bearing and undertaken higher levels of physical activity on their injured limb because less muscle atrophy and higher tendon biomechanics were evident in the treated compared to the control tendons. Development of peritendinous adhesions is a major limitation in tendon healing[5,24,48]; our implants showed reduced peritendinous adhesions.[5,9] The PDS scaffold also had a superior role in decreasing peritendinous adhesions, because it acted as a tendon sheath for the newly regenerated tendons. In addition, it improved the morphologic characteristics of the new tendon compared to the collagen group.

We showed that the prostheses were not rejected by the host; had rejection occurred, more severe and prolonged inflammatory reactions would have been evident, especially at the fibroplasia and remodeling phases of tendon healing. These findings do not support the results of Veillette *et al*.,[15] who showed acute rejection of the implanted acellularized porcine small intestine and filling of the defect area of tendon by an amorphous tissue. Unlike their findings, the new tendon which replaced the implants in the present study was a highly aligned tissue. We used collagen molecules as the sole tissue in producing the collagen implant. All the noncollagenic structures were removed from the bovine tendons, and the architecture of the scaffold was redesigned to accelerate tendon healing. In contrast, Veillette *et al*.[15] only decellularized the xenograft, and did not remove all the antigenic materials from such cadaveric tissue. Therefore, scaffolds of collagen type I are not rejected after implantation in rabbits' tendon defect.

One of the merits of our tissue-engineered prosthesis is its integration with the newly regenerated tissue and its complete absorption and replacement by the newly regenerated tendon. The implant bestows its characteristics on the new tendon but does not remain part of it, as is the case with some other prostheses. For example, after using a poly-L-lactic acid as a prosthesis in a ligament defect model in rabbits, despite excellent biomechanical properties of the repaired area, the implant was not degraded and no new tissue was replaced the scaffold after 16 weeks.[49] Sato *et al*.[50] investigated several different synthetic-based artificial tendons (e.g., polylactic acid), the mechanical properties of which declined over 26 weeks, but were not replaced by new ligaments. In contrast, Gigante *et al*.[51] used a highly aligned bilamellar membrane of type I purified equine collagen in a multi-lamellar conformation to augment a patellar tendon defect model in rabbits. The scaffold was incorporated within the native tendon, in concert with our results. Similarly, Enea *et al*.[52] worked with a patellar tendon defect in a sheep model and used an experimental protocol similar to ours, but with a different type of collagen implant, and they found that it was incorporated into the repaired tissue after 3–6 months.

Despite these beneficial effects of such treatment strategy, the physical and morphological characteristics of the new tendon were still inferior to the intact tendons. The tendon healing process is a complicated and prolonged process, and despite intensive remodeling normal biomechanical characteritstics may never be achieved.[2,9,24] However, 60 DPI is not a very long time for the healing of such a large Achilles tendon defect, as more than 70% of the total Achilles tendon was removed, and healing needs more time to be complete. Longer observation in future studies would be needed to evaluate the final outcome of this treatment strategy.

Biophysical and bioelectrical characteristics of the healing tissues resemble their actual biomechanical and morphological characteristics. We showed that the better morphologically organized tissue exhibits better water binding capacity and electrical resistivity: all these factors correlate with the better load to failure and stress of the healing tissues. Knowledge of these concepts may be valuable when the results of this preliminary study are translated into clinical practice.

This study has tested scaffolds at *in vitro* and *in vivo* levels. However, the success of *in vitro* tests is only the initial requirement for *in vivo* application, and *in vivo* animal experiments are only an approximation to clinical setting.

The anatomical differences between the human and rabbit gastroc soleus-Achilles tendon apparatus could be one of the limitations of the present model. However, we anchored the three strands of the rabbit tendon with the suture, so that the Achilles apparatus acted in the same fashion as the human Achilles tendon, so that the three strands did not have the opportunity of sliding over each other.

Perhaps, by assembling glycosaminoglycans, growth factors and stem cells with such bioimplants, it may be possible to improve the healing response, so that the healing tissue would gain closer characteristics to normal tendons.[41] Before clinical translation, it is highly recommended to test the biocompatibility of the implants by subcutaneous implantation of a small portion in humans. Given the lack of standard methods to reconstruct large Achilles tendon defects, these bioimplants may be applicable in clinical practice in the future.

Conclusion

A tissue engineered tridimensional collagen implant, with or without a PDS covering sheath, improved the healing response. Compared to unassisted tendon healing, the implant was able to produce a newly regenerated tissue of a tendinous nature, which had a lower amount of peritendinous adhesions. This tendon was macro-, micro- and

ultrastructurally, bioelectrically and biophysically superior to the regenerated tissue from unassisted tendon healing; however, these characteristics were inferior to that of the normal tendon at 60 days after tendon injury. Longer periods of observation would be needed to evaluate the final outcome of this treatment strategy. These scaffolds are biocompatible and biodegradable, and might be applied in clinical practice.

Acknowledgment

We thank the Veterinary School, Shiraz University, for financial support and cooperation and much appreciate additional funding through grant ISNF 87020247, from the Iranian National Science Foundation. We are also thankful to Dr A. Mogheiseh, Dr N. Golestani, Dr M. Forood, Dr Y. Aryazand (Department of Clinical Sciences), G. Yousefi, L. Shirvani (Deparment of Pathobiology), A. Safavi (Center of Electron Microscopy), M.R. Solhpoor (Department of Materials Science, Faculty of Engineering), M. Nowroozi, G. Rezaiee, J. Sarikhani (Department of Surgery), all form Shiraz University, Shiraz, Iran, for their technical assistance. This work was supported by the Veterinary School, Shiraz University and the Iranian National Science Foundation (grant ISNF 87020247). The funders had no role in study design, data collection and analysis, decision to publish, or preparation of the manuscript.

Disclosure Statement

The authors declare that no competing interests exist.

References

1. Chalmers, J. Review article: treatment of Achilles tendon ruptures. J Orthop Res **8,** 97, 2000.
2. Moshiri, A., and Oryan, A. Structural and functional modulation of early healing of full-thickness superficial digital flexor tendon rupture in rabbits by repeated subcutaneous administration of exogenous human recombinant basic fibroblast growth factor. J Foot Ankle Surg **50,** 654, 2011.
3. Maffulli, N., Spiezia, F., Testa, V., Capasso, G., Longo, U.G., and Denaro, V. Free gracilis tendon graft for reconstruction of the Achilles tendons. J Bone Joint Surg Am **94,** 906, 2012.
4. Ronel, D.N., Newman, M.I., Gayle, L.B., and Hoffman, L.A. Recent advances in the reconstruction of complex Achilles tendon defects. Microsurgery **24,** 18, 2004.
5. Khanna, A., Friel, M., Gougoulias, N., Longo, U.G., and Maffulli, N. Prevention of adhesions in surgery of the flexor tendons of the hand: what is the evidence? Br Med Bull **90,** 85, 2009.
6. Oryan, A., Moshiri, A., Meimandiparizi, A.H., and Raayat Jahromi, A. Repeated administration of exogenous sodium-hyaluronate improved tendon healing in an *in vivo* transection model J Tissue Viability **21,** 88, 2012.
7. Oryan, A., and Moshiri, A. A long term study on the role of exogenous human recombinant basic fibroblast growth factor on the superficial digital flexor tendon healing in rabbits. J Musculoskelet Neuronal Interact **11,** 185, 2011.
8. Metz, R., van der Heijden, G.J., Verleisdonk, E.J., Kolfschoten, N., Verhofstad, M.H., and van der Werken, C. Effect of complications after minimally invasive surgical repair of acute Achilles tendon ruptures: report on 211 cases. Am J Sports Med **39,** 820, 2011.
9. Shearn, J.T., Kinneberg, K.R., Dyment, N.A., Galloway, M.T., Kenter, K., Wylie, C., and Butler, D.L. Tendon tissue engineering: progress, challenges, and translation to clinic. J Musculoskelet Neuronal Interact **11,** 163, 2011.
10. Dy, C.J., Hernandez-Soria, A., Ma, Y., Roberts, T.R., and Daluiski, A. Complications after flexor tendon repair: a systematic review and meta-analysis. J Hand Surg Am **37,** 543.e1, 2012.
11. Lapidus, L.J., Ray, B.A., and Hamberg, P. Medial Achilles tendon island flap—a novel technique to treat reruptures and neglected ruptures of the Achilles tendon. Int Orthop **36,** 1629, 2012.
12. Peterson, R.K., Shelton, W.R., and Bomboy, A.L. Allograft versus autograft patellar tendon anterior cruciate ligament reconstruction: a 5-year follow-up. Arthroscopy **17,** 9, 2001.
13. Hasslund, S., Jacobson, J.A., Dadali, T., Basile, P., Ulrich-Vinther, M., Søballe, K., Schwarz, E.M., O'Keefe, R.J., Mitten, D.J., and Awad, H.A. Adhesions in a murine flexor tendon graft model: autograft versus allograft reconstruction. J Orthop Res **26,** 824, 2008.
14. Sun, K., Tian, S., Zhang, J., Xia, C., Zhang, C., and Yu, T. Anterior cruciate ligament reconstruction with BPTB autograft, irradiated versus non-irradiated allograft: a prospective randomized clinical study. Knee Surg Sports Traumatol Arthrosc **17,** 464, 2009.
15. Veillette, C.J., Cunningham, K.D., Hart, D.A., Fritzler, M.J., and Frank, C.B. Localization and characterization of porcine patellar tendon xenograft antigens in a rabbit model of medial collateral ligament replacement. Transplantation **65,** 486, 1998.
16. Allman, A.J., McPherson, T.B., Badylak, S.F., Merrill, L.C., Kallakury, B., Sheehan, C., Raeder, R.H., and Metzger, D.W. Xenogeneic extracellular matrix grafts elicit a TH2-restricted immune response. Transplantation **71,** 1631, 2001.
17. Bartlett, R.J., Clatworthy, M.G., and Nguyen, T.N.V. Graft selection in reconstruction of the anterior cruciate ligament. J Bone Joint Surg Br **83-B,** 625, 2001.
18. Longo, U.G., Lamberti, A., Maffulli, N., and Denaro, V. Tendon augmentation grafts: a systematic review. Br Med Bull **94,** 165, 2010.
19. Chen, J., Xu, J., Wang, A., and Zheng, M. Scaffolds for tendon and ligament repair: review of the efficacy of commercial products. Expert Rev Med Devices **6,** 61, 2009.
20. Hsu, S.L., Liang, R., and Woo, S.L. Functional tissue engineering of ligament healing. Sports Med Arthrosc Rehabil Ther Technol **2,** 12, 2010.
21. Maffulli, N., Longo, U.G., and Loppini, M. New options in the management of tendinopathy. Open Access J Sports Med **1,** 29, 2010.
22. Anselme, K., Bacques, C., Charriere, G., Hartmann, D.J., Herbage, D., and Garrone, R. Tissue reaction to subcutaneous implantation of a collagen sponge. A histological, ultrastructural, and immunological study. J Biomed Mater Res **24,** 689, 1990.
23. Whitlock, P.W., Smith, T.L., Poehling, G.G., Shilt, J.S., and Van Dyke, M. A naturally derived, cytocompatible, and architecturally optimized scaffold for tendon and ligament regeneration. Biomaterials **28,** 4321, 2007.
24. Sharma, P., and Maffulli, N. Tendon injury and tendinopathy: healing and repair. J Bone Joint Surg Am **87,** 187, 2005.
25. Sharma, P., and Maffulli, N. Biology of tendon injury: healing, modeling and remodeling. J Musculoskelet Neuronal Interact **6,** 181, 2006.

26. Oryan, A., and Shoushtari, A.H. Histology and ultrastructure of the developing superficial digital flexor tendon in rabbits. Anat Histol Embryol **37,** 134, 2008.
27. Oryan, A., Moshiri, A., and Meimandiparizi, A.H. Effects of sodium-hyaluronate and glucosamine-chondroitin sulfate on remodeling stage of tenotomized superficial digital flexor tendon in rabbits: a clinical, histopathological, ultrastructural, and biomechanical study. Connect Tissue Res **52,** 329, 2011.
28. Foltran, I., Foresti, E., Parma, B., Sabatino, P., and Roveri, N. Novel biologically inspired collagen nanofibers reconstituted by electrospinning method. Macromol Symp **269,** 111, 2008.
29. Wray, L.S., and Orwin, E.J. Recreating the microenvironment of the native cornea for tissue engineering applications. Tissue Eng Part A **15,** 1463, 2009.
30. Dubey, N., Letourneau, P.C., and Tranquillo, R.T. Neuronal contact guidance in magnetically aligned fibrin gels: effect of variation in gel mechano-structural properties. Biomaterials **22,** 1065, 2001.
31. McCall, A.S., Kraft, S., Edelhauser, H.F., Kidder, G.W., Lundquist, R.R., Bradshaw, H.E., Dedeic, Z., Dionne, M.J., Clement, E.M., and Conrad, G.W. Mechanisms of corneal tissue cross-linking in response to treatment with topical riboflavin and long-wavelength ultraviolet radiation (UVA). Invest Ophthalmol Vis Sci **51,** 129, 2010.
32. Stillaert, F.B., Di-Bartolo, C., Hunt, J.A., Rhodes, N.P., Tognana, E., Monstrey, S., and Blondeel, P.N. Human clinical experience with adipose precursor cells seeded on hyaluronic acid-based spongy scaffolds. Biomaterials **29,** 3953, 2008.
33. Siritientong, T., Srichana, T., and Aramwit, P. The effect of sterilization methods on the physical properties of silk sericin scaffolds. AAPS Pharm Sci Tech **12,** 771, 2011.
34. Tsai, S.P., Hsieh, C.Y., Hsieh, C.Y., Wang, D., Huang, L.L., Lai, J., and Hsieh, H. Preparation and cell compatibility evaluation of chitosan/collagen composite scaffolds using amino acids as crosslinking bridges. J Appl Polym Sci **105,** 1774, 2007.
35. Oryan, A., Moshiri, A., and Meimandiparizi, A.H. Short and long terms healing of the experimentally transverse sectioned tendon in rabbits. Sports Med Arthrosc Rehabil Ther Technol **4,** 14, 2012.
36. Oryan, A., Moshiri, A., and Raayat, A.R. Novel application of Theranekron® enhanced the structural and functional performance of the tenotomized tendon in rabbits. Cells Tissues Organs **196,** 442, 2012.
37. Oryan, A., and Moshiri, A. Recombinant fibroblast growth protein enhances healing ability of experimentally induced tendon injury *in vivo*. J Tissue Eng Regen Med 2012. [Epub ahead of print]; DOI: 10.1002/term.1534. http://onlinelibrary.wiley.com/doi/10.1002/term.1534/abstract. Accessed May 17, 2013.
38. Poltawski, L., and Watson, T. Bioelectricity and microcurrent therapy for tissue healing–a narrative review. Phys Ther Rev **14,** 104, 2009.
39. Bartone, F.F., Shervey, P.D., and Gardner, P.J. Long term tissue reponces to catgut and collagen sutures. Invest Urol **13,** 390, 1976.
40. Pieper, J.S., Oosterhof, A., Dijkstra, P.J., Veerkamp, J.H., and van Kuppevelt, T.H. Preparation and characterization of porous crosslinked collagenous matrices containing bioavailable chondroitin sulfate. Biomaterials **20,** 847, 1999.
41. Ping Ooi, C., and Cameron, R.E. The hydrolytic degradation of polydioxanone (PDSII) sutures. Part II: Micromechanisms of deformation. J Biomed Mater Res **63,** 291, 2002.
42. Postlethwaite, A.E., Seyer, J.M., and Kang, A.H. Chemotactic attraction of human fibroblasts to type I, II, and III collagens and collagen-derived peptides. Proc Natl Acad Sci U S A **75,** 871, 1978.
43. Saeidi, N., Guo, X., Hutcheon, A.E., Sander, E.A., Bale, S.S., Melotti, S.A., Zieske, J.D., Trinkaus-Randall, V., and Ruberti, J.W. Disorganized collagen scaffold interferes with fibroblast mediated deposition of organizedextracellular matrix *in vitro*. Biotechnol Bioeng **109,** 2683, 2012.
44. Oryan, A., Goodship, A.E., and Silver, I.A. Response of a collagenase-induced tendon injury to treatment with a polysulphated glycosaminoglycan (adequan). Connect Tissue Res **49,** 351, 2008.
45. Magra, M., Hughes, S., El Haj, A.J., and Maffulli, N. VOCCs and TREK-1 ion channel expression in human tenocytes. Am J Physiol Cell Physiol **292,** C1053, 2007.
46. Sharma, P., Hughes, S., El Haj, A., and Maffulli, N. Expression of the two pore domain potassium channel TREK-1 in human intervertebral disc cells. Curr Stem Cell Res Ther **7,** 266, 2012.
47. Gupta, K., Gupta, P., Singh, G.K., Kumar, S., Singh, R.K., and Srivastava, R.N. Changes in electrical properties of bones as a diagnostic tool for measurement of fracture healing. Hard Tissue 2 (1), 3. Available online at: www.oapublishinglondon.com/images/article/pdf/1363433172.pdf
48. Andia, I., Sanchez, M., and Maffulli, N. Tendon healing and platelet-rich plasma therapies. Expert Opin Biol Ther **10,** 1415, 2010.
49. Nishimoto, H., Kokubu, T., Inui, A., Mifune, Y., Nishida, K., Fujioka, H., Yokota, K., Hiwa, C., and Kurosaka, M. Ligament regeneration using an absorbable stent-shaped poly-L-lactic acid scaffold in a rabbit model. Int Orthop **36,** 2379, 2012.
50. Sato, M., Maeda, M., Kurosawa, H., Inoue, Y., Yamauchi, Y., and Iwase, H. Reconstruction of rabbit Achilles tendon with three bioabsorbable materials: histological and biomechanical studies. J Orthop Sci **5,** 256, 2000.
51. Gigante, A., Busilacchi, A., Lonzi, B., Cecconi, S., Manzotti, S., Renghini, C., Giuliani, A., and Mattioli-Belmonte, M. Purified collagen I oriented membrane for tendon repair: an *ex vivo* morphological study. J Orthop Res **31,** 738, 2013.
52. Enea, D., Gwynne, J., Kew, S., Arumugam, M., Shepherd, J., Brooks, R., Ghose, S., Best, S., Cameron, R., and Rushton, N. Collagen fibre implant for tendon and ligament biological augmentation. *In vivo* study in an ovine model. Knee Surg Sports Traumatol Arthrosc **21,** 1783, 2012.

Address correspondence to:
Nicola Maffulli MD, MS, PhD, FRCP, FRCS (Orth), FFSEM
Department of Musculoskeletal Medicine and Surgery
Faculty of Medicine and Surgery
University of Salerno
Salerno, Italy

E-mail: n.maffulli@qmul.ac.uk

Received: January 25, 2013
Accepted: August 30, 2013
Online Publication Date: October 14, 2013